Spectrum of Engineering Sciences
ISSN (e) 3007-3138 (p) 3007-312X Volume 4, Issue 6, 2026

A NON-INVASIVE METHOD FOR BRAIN TUMOR DETECTION USING COMPUTER VISION AND DEEP LEARNING TECHNIQUES

Abid Farooq[1], Hina Shafique[2], Aqsa Khursheed[3], Anum Saher[4], Shafqat Ali[5], Ghulam Gilanie[*6]

[1,2,3,4,*6]*Department of Artificial Intelligence, Faculty of Computing, The Islamia University of Bahawalpur, Pakistan.*
[5]*Department of Mathematics, Faculty of Physical and Mathematical Sciences, The Islamia University of Bahawalpur, Pakistan*

[1]abid.farooq12@gmail.com, [2]hinach1912@gmail.com, [3]aqsakhursheedbwp@gmail.com, [4]saheranum1@gmail.com, [5]shafqat.ali@iub.edu.pk, [*6]ghulam.gilanie@iub.edu.pk

DOI: https://doi.org/10.5281/zenodo.20845161

Keywords
Brain Tumor Detection, Computer Vision, Deep Learning

Article History
Received: 24 April 2026
Accepted: 06 June 2026
Published: 21 June 2026

Corresponding Author: *
Ghulam Gilanie

Abstract

In the brain tumor diagnosis technique, the study of the brain MR image is supportive. For human life, cancer and tumors are deadly and damaging diseases. In the world of the Biocomputing field, this study is an additional struggle to tell about the position of image classification. A brain tumor is an uncontrolled growth of cancerous and non-cancerous cells in the brain. A brain tumor may be malignant or benign. The brain tumor symptoms depend upon the size of the tumor, location, and its type. The brain tumor is classified into two different types: a secondary brain tumor and a primary brain tumor. The organs of the brain cell where the tumor is located and grows up from these cells; this type is called a primary brain tumor. A cell of the tumor that belongs to another part of the body and may extend rapidly into the brain is called a secondary brain tumor. To evaluate and check the competence of the suggested model, the MATLAB tool is used. In this research, the dataset is collected from the Bahawalpur Victoria Hospital (BVH). It is concluded that this proposed method is better than other existing methods in terms of computation time after analyzing the results. Properties of feature extraction, i.e., mean, entropy, standard deviation, variance, connectivity, and many other features, are obtained. I have set a central tendency value in mean, standard deviation, and variance. If the value is less than the central tendency, that refers to a primary brain tumor; otherwise, it will be a secondary brain tumor. I have compared the results from other proposed methods. our proposed technique gives better results with an accuracy of 92.93. In the future, further classifier techniques may reach to find better results. Brain tumors, especially glioma, meningioma, and residual tumors, are common with a low survival rate. Clinically, they are identified on MRI scans and are classified after invasive methods. Spinal tap and biopsy are the methods used to determine the type of brain tumor. In this research work, a CNN-based architecture has been proposed to classify brain tumors in a non-invasive manner. Three classes, i.e., glioma, meningioma, and residual tumor, have been classified. The dataset has been collected from Bahawal Victoria Hospital, Bahawalpur, Pakistan. Experiments have been performed in different ways: 1) processing of as it is images present in the dataset, 2) processing the tumor segmented images, and 3)

processing the large number of tumor segmented images. Experiment no. 01, experiment no. 02, experiment no. 03, experiment no. 04, experiment no. 05 and experiment no. 06 have achieved the accuracy as 66.13%, 80.93%, 88.07%, 91.33%, 92.00%, and 92.93% respectively. The proposed method has achieved an accuracy of 92.93%, which is high compared to the state-of-the-art methods. It has been experimentally proven that increasing the number of images has increased the achieved accuracy. In future work of this research, all other brain tumor types will be classified. It is further aimed that will four WHO grades will also be classified using a non-invasive method to replace biopsy and spinal tape methods.

1.1 INTRODUCTION

In the brain tumor diagnosis technique, the study of the brain MR image is supportive. For human life, cancer and tumors are a death-defying and damaging disease. In the world of the Biocomputing field, this study is an additional struggle to tell about the position of image classification. Improved the method of disease diagnosis image classification technique is competently. For the image classification,some techniques have been presented like fuzzy C-mea,Boltsman,random forest, support vector machine (SVM) and many others. Thislearning suggested a method in which grey scaled classification method is used with deep neural networks technique. In the least computational time these arrangements of two technique is giving a well outcome.

Cell is the basic unit of life and because of which all living things are made. Cells are unicellular and multicellular in nature. Unicellular cells are itself an organism such as yeast and bacteria. Similarly, some cells cooperate with some other cells and converted into a building block unit like human beings. As individual unit the cells are capable of generating its own nutrients, many kinds of molecules, generating energy and multiplying itself for the production of similar cells. Cells are actually looked as an enclosed capsule like structure in which many chemical reactions take place at a time [1-13].

Blood cells play a leading role from disseminating oxygen in the whole body to the fight against infection. RBCs governs blood type and transport oxygen to the cells. WBCs provides immunity by killing the pathogens. Platelets help in clotting the blood and reduce the blood loss due to blood vessel damage [14, 15].

Muscle cells established muscle tissues that are important for the body movement. Skeletal muscle tissues are connected to bones and make them enable for voluntary movement. These are covered by the connective tissues for the protection of muscle fiber. Cardiac muscled help out in the contraction of heart and are interlinked by discs which controls the heartbeat. Smooth muscles act as a lining agent and lines body cavities and also form the wall of body organs [16-25].

Nerve cells are the base of the nervous system. These cells send indicator to the brain, spinal cord and other body parts. Nerve projection consists of the axons and the dendrites that are helpful in transmitting signals [26-46].

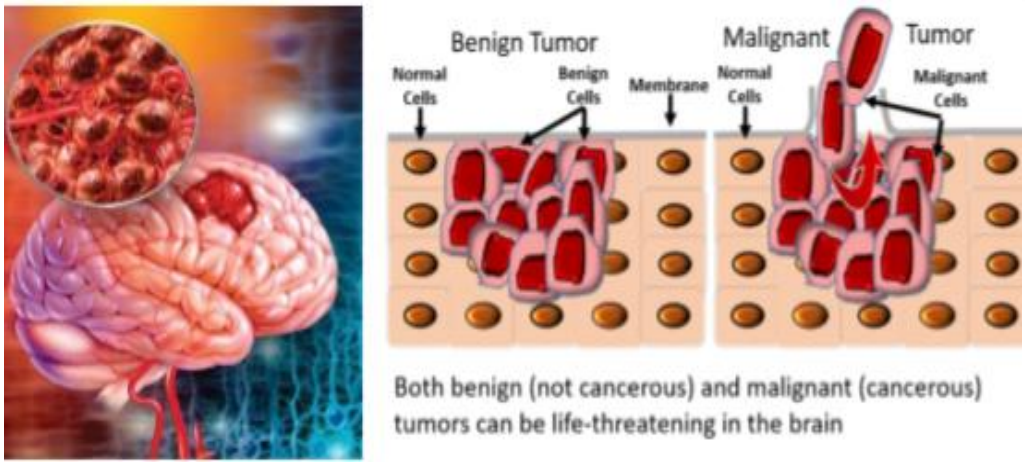

(A) (B)

Figure 1. In this figur, 'A' and 'B' are the example of brain tumor images[47].

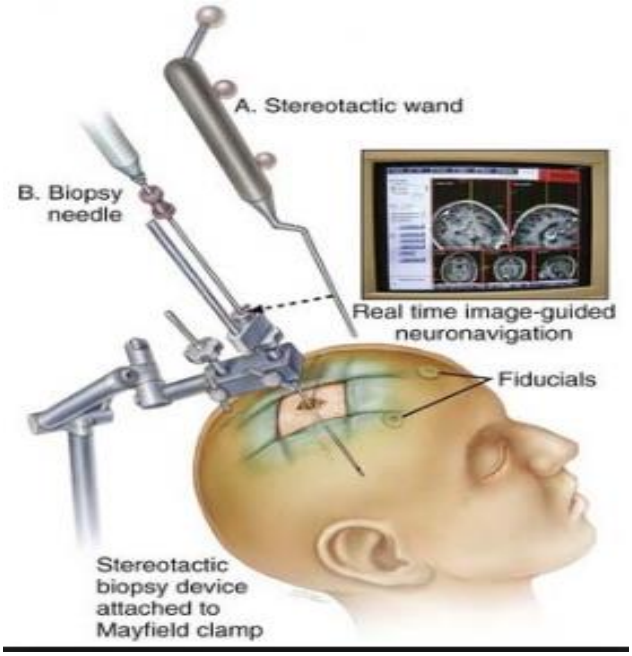

Figure 1. In this picture biopsy process of the brain is shown

To get brain images different imaging techniques are used [48-54]. In the field of medical computed tomography(CT) scan is an imperative imaging technique and generally the interval reduced to the segment of it and the information is make available in seconds. As compare with X-rays, CT scan provides a more clear information [55-73].

PET: Positron emission tomography is a technique and a scanner identified. An idea of the role of brain and brain's activity has acquired from this technique. Harmful and cost-effective materials are used in this method.

X-rays: X-rays is another imaging techniques, about the organ. If X-ray is used several time in the same place and body it may cause skin cancer. However, this procedure is costly and relaxed to use.

1.2 MR Image Characteristics of the brain Tumor

Imaging procedure of an MRI image is extra beneficial than then X-rays[74]. MR images don't use harmful radiation and provide enough information to diagnose diseases and making decisions to doctors [75]. Difference between delivering a pulse RF echo signal received. TR time (repeat) time reception among uninterrupted pulsates is applied in the identical arrangement.

T1-weighted images

T1-weighted images comprise the black presence of fluid and CSF. As compared with white matter (WM) gray matter (GM) is mor darker. In this case of brain images structure T1 has given a more better result and in this type, plump looks brighter [76]. TR and TE time (TE = 14msec and TR = 500msec) is to produce the images in short (using longitudinal relaxation).

Images of T2-weighted

T2-weighted images have appeared bright when the intensity of fluid and CSF contain a higher signal for that reason it is compared with tissue [77]. For longtime T2 is used (TR=4000msec, TE=19msec) to produced images from TR and TE (traverse relaxation). T2 images is brighter for fluid and water and ideal to the edema tissue.

FLAIR

Flair and T2 weighted images have the same aspect but abnormalities remain brighter when it has attenuated from CSF fluid. The cerebral edema has good for imaging. It has used for producing images TR and TE time has very long (TR=9000msec, TE=114msec) for producing images[78].

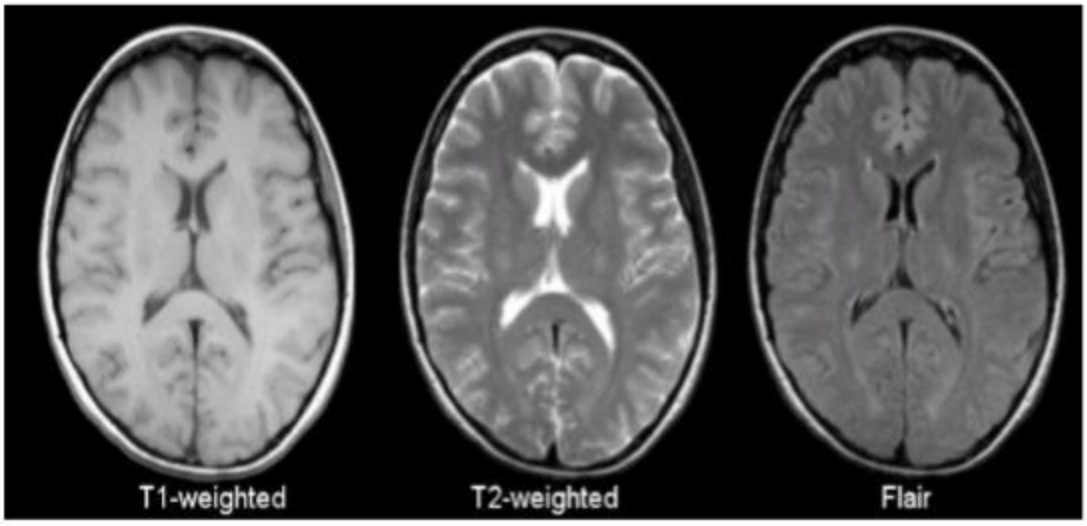

Figure 3. In this fig.different images technique of MRI are shown[77].

Table 1: On the basis of different tissues the differences among the T1,T2 and FLAIR are represented which are given below.

Tissues	T1-weighted	T2-weighted	FLAIR
CSF	Dark	Bright	Dark
White matter	Light	Dark grey	Dark grey
cortex	Grey	Light grey	Light grey
Fat(within bone marrow)	Bright	Light	Light
Inflammation (impurity)	Dark	Bright	Bright

With the help of this above table, the different feature of T1, T2 and FLAIR are illustrated.

The research objective is to confidentally classify the brain tumor types to reduce doctor burden, leaving the most complex diagnoses to them.

There are following some objectives in the perception of research:

a) To provide a computer based fully automated way for grading of brain tumour from brain MRS slices.

b) To reduce the calculation/time in tumour grading.

c) To design a procedure that is more accurate and robust than the approaches already exists.

d) To investigate artificial intelligence, image processing, computer vision, and machine learning established methods, which might be used as an alternate to a dangerous biopsy procedure.

In this study brain tumor can be diagnosed more efficiently and accurately is associated in the field of image treating by presenting. This study involved another task along this model which is given below.

- An analysis of the alignment and classification procedure and discuss of it with other techniques..
- With grey scaled segmentation method a model of DNN is proposing.
- For suitable and effective treatment improved a diagnosis method of the brain tumor.

In this research study, review of the earlier work is discussed. Magnetic resonance image (MRI) get a good result for the treatment preparation and upgrading deep neural networks. This study provide helps for doctors, surgeons and radiologist in the diagnosis of disease. In the field of image processing, this study will contribute efficiently [79-82].

The outcome of the conducted research as an application will assist several medical units. In cancer diagnostic and cure hospitals and institutes it will help in diagnosis, classification and grading of brain tumor so that more affordable treatment planning be executed.

The breakdown of this thesis is planned as follows. section 2 defines the background. In section 3, reviewed literature has been positioned. While methodology has been placed in section 4. Section 5 has results obtained through the proposed method along with their discussions. Conclusion along with future remarks is presented in the last chapter of this research.

2 Literature review

The researcher Muhammad Naeem Tahir has purposed and study on the characterization and classify MRI of brain tumor using technique grayscaled segmentation and Deep Neural Networks(DNN). He has used MRI techniques for a diagnosed brain tumor. For images classification and separation his a lot of struggle has been done [77].

The authors Saurabh Shah et. al., has suggested and explain the brain tumor classification from MRI using excellent method Computational Intelligent Techniques [83].

The investigator A Damayanti et.al has proposed an excellent work for the classification brain tumor based on the Magnetic Resonance Image(MRI) of the brain using techniques neuro-fuzzy mode and wavelet energy feature. You can organize the brain tumor classification method to correct conclusion and the right treatment and the right brain tumor treatment method. In this study, the technique of classification for brain tumor disease type arrangement, namely, Alzheimer's disease, glioma, cancer, using an ANFIS and energy coefficient. Advance phases[84] in the classification of MRI brain images are the reduction of the feature, techniques of classification and a feature extraction. As a result of vector calculation feature extraction for all wavelets falling off. Low falling method feature by using vector approximation of energy transactions. As a result of the reduction in feature to 100 power plants each feature 1 x 52 pixels. This will contribute to the vector classification using ANFIS with FLVQ grouping procedure, LM backpropagation and fuzzy C Mean. The success rate of MRI brain tumor images as a percentage have achieved at 100% appreciation using FLVQ, LM backpropagation and ANFIS.

The authors Noramalina Abdullah et.al has worked on the brain tumor MRI brain images classification using good method support vector machine (SVM). For the classification of brain tumor, they have used a techniques MRI and SVM. It was the initial diagnosis and treatment evaluation tools to analyze brain MRI (magnetic resonance imaging) [47].

The authors Janki Naik et.al have suggested and worked on the brain tumor classification and detection using tree decision in the brain MRI procedure. Here, they present some experiments to detect the tumor in MRI images. It was done in the previous step using the average processing filter operation and the extracted features using texture feature extraction techniques. Using features extracted from CT images mine Association rules. The proposed method is used for the classification of medical images for diagnosis. In this system, they were going to use an algorithm "decision tree" classification. The proposed method improves the efficiency of traditional image mining techniques. There, the results are compared with the classification Naive Bayesian algorithm[85].

The authors Khalid Usman and Kashif Rajpoot et.al has classified the brain tumor using techniques machine learning apparatus and wavelets from multi-modality Magnetic Resonance Images(MRI). They obtained datasets from MICCAI Brat's datasets which are publically available. They validated the outcome standard evaluation measure such as the Dice coefficient and the Jaccard coefficient. They obtained a result for the HG and LG is the proposed method for complete high-grade HG is 0.88 and for complete low-grade LG is 0.81. By the use of different classifiers (KNN, RF, Ada Boost M_2 and Rus Boost). For HG and LG on real data set the leave-one-out cross-validation is performed separately. The tumor is classified into three regions; complete tumor, core tumor and enhancing tumor from the further performed detailed classification. From the other existing techniques, the proposed techniques give comparable and favorable results [86].

The investigated James Fink et. Al has used a technique radiation necrosis relevance with respect for the treatment of primary and secondary brain tumor. They obtained data set from computed tomography (CT) and MRI. There is no standard imaging method to discriminate among the high-grade gliomas recurrence, radiation necrosis, an advance physiologic MRI technique and the F-Flourodeoxy glucose positron emission tomography radiotracer is an area of active

investigations. The validated their outcome on the standard additional cellular mechanisms in the CNS such as the hypoxia-induced factor(HIF) and vascular endothelial growth factor (VEGF). These factors might start of the cataract outcome of radiation necrosis which is expressed by astrocyte. While an overstated reaction to radiation might apparent as necessitate treatment, clinically significant mass effect, regardless the radiation necrosis contained inside the RT target is commonly imaginary to the treatment outcome relatively than the obstacle. Radiation necrosis is treated may be medically or surgically. Although the compelling evidence-based foundation has neither modality[87].

The researcher Muhammad Havaei, Axel Davy et.al has segmented the brain tumor with deep neural networks [88]. They obtained datasets from BRATS which is publically available. They validated their outcome on the standard evaluation system. Dice, sensitivity and specificity are compared for each tumor region. The result for Dice, Specificity and Sensitivity is 0.84, 0.95 and 0.77 respectively. Magnetic resonance Images (MRI) modality procedure is often used for the solution of more than one e.g contrast imaging, diffusion MRI(dMRI), fluid attenuation inversion recovery(FLAIR) and proton density(PD) pulse sequence. The approaches their convolution neural network, BRATS datasets deficiency resolve in the third measurement. The separation portion by portion from the axial view supposed performing. The feedback level surface usually comprises of feature maps of the earlier sheet in the succeeding sheet. Convolution layer consists of three steps for the computing a feature map which is these following convolution of kernels, non- linear activation function and max pooling. The BRATS 2015 challenge took part by using the best performing method. Training datasets comprise the BRATS 2015 with high-grade gliomas are 220 subjects and with low-grade gliomas are 54 subjects. For the testing of high and low grade gliomas there 53 subjects are mixed. The uppermost performance method in BRATS' 12 and BRATS'13 segmented results of brain tumor is compared by voting. In the ranked method both first and second on complete tumor and tumor central class and acquire good results on the energetic tumor. This technique has also a smaller amount of outliers then greatest further methodologies.

The authors Kimia Rezaei and Hamad agahi have classified and segment the malignant and benign brain tumor using the SVM with weighted kernel width. They obtained datasets from the co-occurrence gray-level matrix and run length dominant gray-level matrix method which is publically available. They validated their outcome on standard evaluation mean such as T-test and the Weighted Gaussian RBF kernel. The evaluation of segmentation performance by the computation segmentation accuracy.

Segmentation accuracy = (No. of matched pixels / from Ground truth the total no.of tumor pixels)×100

On the basis of the error rate, the classifier's accuracy is evaluated. The segmentation accuracy of 10 patient with 100 slices, the average accuracy segmentation for the malignant slices(50) is 89.182 and for benign slices(50) is 88.816. By the sensitivity and specificity, the classification accuracy effective is measured. The classification of KNN and SVM is 74% and 76% respectfully, WSVM performed good with the accuracy of 77%. The proposed method can be applied for future work such as magnetic resonance image (MRI) to the other types of imaging I and even can be used in other part of the body for classification and segmentation of tumor[89].

The researcher Justin Paul has [90] purposed of the study is to classify the brain tumor by deep learning machine for the different typesbrain tumor images: meningioma, glioma and pituitary. He obtained datasets from T_1-weighted contrast-enhanced images (CE-MRI) with three sets of images categorized: axial, coronal and sagittal images which are publically available. Using the more general method of the neural network and by adding images of the brain without tumors this research improves on previously presented results. Furthermore; applying a neural network to medical images has an implication of faster and more precise diagnoses. The main contribution of this research paper are as follows; create a more generalized method for classification of brain

tumor by using deep learning. Analyze the application of tumorless brain images on the classification of the brain tumor. Empirically evaluate the given datasets from the neural network with per images accuracy and per patient accuracy. Images data was preprocessed in several forms. Each form of preprocessing is described as Vanilla Data preprocessing, Images, Location and Tumor Zoom. This can especially improve meningioma tumors which caused neural network the most difficult in classifying.

3 Methodology

The research methodology of this learning is contained in this part of as it is stated in heading. Additional information of the outline is provided in this section of the research approach, research technique, basis of datasets, research process, data types study, the moral thoughts and the limitation of this research study.

3.1.1 Collection for Analysis and of Relevant Data

This learning is succeeding mutually graphic and investigational learning. Associated facts determination can be collected from concluded records, articles, research paper, thesis magazine andfrom net source. For analysis materials, all the study will be settled and composed. To reach at particular final arguments the materials and subjects will discuss with the instructor for comfort.

In the problem statement, the argument and study will lead to the identification.

Solve the Problem of the Proposed Model

Problem statement has recognized to bargain the explanation will be in the succeeding period. The well and well-organized results have acquired from this suggested work.

Proposed Model for Implementation

The results are obtained by using MATLAB toolbox and application of these suggested techniques and model.

This stage will lead the concluding brief argument of the complete study and define the references of it. This suggested work discuss its improvement and the efficiency which will also be stated for the next investigation in future work.

This technique will depend on the literature based learning. It means ideally investigation of that methodology which contains arguments and selection of theoretical materials and imaginative materials and these theories give a complete evaluation in the context, by proposing perfect solution try to decide and finding main issues. This study motivate will be in empirically.

3.1.2 Datasets

The relevant data which is used and collected from internet source(books, topic, article, research paper and thesis). In the earlier research, the data of brain tumor will be composed for classification method and will be applied for assessment on the basis of unlike feature like

- Rate of accuracy
- Technique (which can be used for imaging processing)

The dataset of MR Images will get from BVH. Dissimilar type of MR Images will be obtainable according to necessity.

3.1.3 Technique for Data Analysis Procedure

The collected data will be checked and connected by different features. A specific method or procedure used to examine magnetic resonance images (MRI) of the brain. The method to be used to classify the MR image of the proposed model are the neural network. Neural networks are often normal "two hidden layers that use a lot of managed or predicted classification. Deep learning design neural networks(NN) are different from neural networks "normal" because of the extra hidden layers as shown in FIGURE 3.1. Neural network calculation is perfect using deep learning after the nature of the human brain. According to the human mind, the deep neural networks(DNN) is also the basics of editing (neuron). Explain the important elements of neural networks. Processing is divided into groups called classes. DNN consists of three layers, which are the input and output layer and the hidden layers. When images develop before and give input with deep neural networks(DNN) the output image format trend indicators in the form of slashes, one for

each purpose. The class with the highest score we refer to the category that is most likely to be targeted in the picture. Deep neural networks(DNN) training aims to monitor the weights that make full use of the scores right category and to lose masses of untrue accusation. During the training of neural networks, is measure the degree gap between the corrected results is called lose and calculated results are losing, the goal is a hidden layer of normal loss of losing more than a wide range of training.

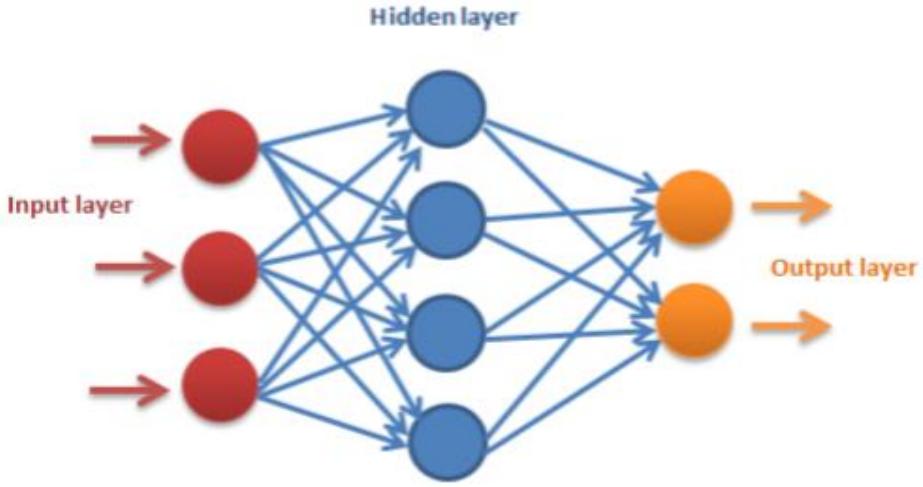

Figure 4. Deep neural networks (DNN) stucture in layers are shown in [77]this picture.

Deep learning not just the opposite of "normal" NN (neural networks) but support vector machine (SVM), which is more common and the sorting algorithm because this can train with the style of uncensored or uncensored mutual supervision and supervision functions of learning. The previous classification, filtered images to increase the image quality that will help MRI. To increase and de-noise the quality of brain MRI images this separation will help. Separation of gray scale will be used for further processing to perfect images and make them into classification systems and improved results. Confidential results will help to calculate the size of tumors and identified the brain tumor images by resolution of MRI image and will use the picture of the Interior of the domain account. Will break into pixels on a confidential basis and to calculate the rows and columns, that allow the algorithm.

3.1.4 Analysis Tool (Software)

Matlab tool is used for investigation and analysis process. For calculation of math works Matlab tool can be used to evaluate and checked the compmetence of the suggested model and algorithms. [91]. To design and analyze the system MATLAB is used. MATLAB is used for the digital image procession, machine learning, control design, computer vision, communication and signal processing etc. Classification performance is analyzed from MATLAB. The plotting of data and function, implementations of algorithms, matrix manipulations and interface with various programming language MATLAB allows.

3.1.5 Computation Accuracy

The algorithm of performance can be evaluated in terms of specificity, accuracy and sensitivity. Matrix violation definitions TP (true positive), TN (true negative), FN(false negative), FP(false positive) and planned the expected result and true results to calculate the accuracy and sensitivity and specificity of ground truth are displayed in the below table 3.1 [92].

Table 2. Confusion matrix defining the term TN, FP, FN, and TN

Expected out comes	Ground truth		
	Positive	Negative	Row total
Positive	TP	FP	TP+FP
Negative	FN	TN	FN+TN
Column total	TP+FN	FP+TN	TP+FP+FN+TN

Where n is the number of true positives, used to indicate the total number of abnormalities that are classified correctly, TN is no real negatives, used to refer to normal cases classified correctly,FP is a false positive and is used to indicate abnormalities correct or confidential, when it is actually normal cases and the number of false negatives is the national front, is used to refer to normal confidentiality or detection error, when in fact anomalies [3], every one of these results parameters are calculated using the total number of sample for detection of tumor. Precision quality percentage parameter in the percentage of the total of cases that have been categorized correctly is normal and normal rank and are normally classified as usual from the total number of cases considered [93].

3.1.6 Consideration of Ethicals

Ethical anxieties and difficulty are not unusual in patients with brain tumors, as well as for the disclosure. It is important to have knowledge of the principles, in addition to the theory of morality in favor of patients, as are the decisions of life except for death. Moral principles over most of the respect of sovereignty and justice and abandoned. To resolve ethical questions, it is important to follow all the appropriate rules and principles in patients neurology, for example, Discuss diagnosis or prediction. Image quality is provided for analysis and diagnosis. What will the precise calculations with the rules and principles of research, as well as the techniques for decision-making, to improve your capability to make expressive selections.

3.1.7 Limitation of this Research

Following limitation of this research are given below

- ❖ The material which is used in this research from previous research will be among the duration of 2012 to 2018 (last seven years).
- ❖ For experiment, the dataset will be used in the limited number.
- ❖ Through Matlab analysis tool this prop[osed model will be justified.

3.2 Methods and Materials

3.2.1 Image Preprocessing and Data Aquisition

Experiments conducted with consideration for the institutional review board (IRB). All tests on kids are permitted from parents written models. Acquired T1, T2 and pictures from MRI diffusion weighted 10 healthy children using Siemens 3T MR scanner on the head only. These guys were asleep and consistent with the safety of the ear, and their heads are protected for free install method during scanning. Images sagittal slices a T1 144 realized with TE/TR 1900/MS, 4.38 ° face angle 7 use analysis 1 x 1 x 1 mm3. T2 images a key slides 64 checked with TE/TR as 7380/119ms, facial angle 150 ° to use precision 1.25 x 1.25 x 1.95 mm3. DWI(diffusion-weighted images) having axial slices 60 are acquired 7680/82ms with TR/TE as using of $2x2x2mm^3$ resolution and non-linear 42 dispersion grades with a diffusion-weighted of 1000 s/mm2.

Fractional anisotropy (FA) images and T2 weighted images, the resulting distortion correction, first well compatible with T1 and

Furthermore the image samples until the private network with an accuracy of 1 x 1 x 1 mm3. Rescanning is performed when the data is transferred in a logical move or simple objects [94]. Then I can improve functional density inhomoginity at T1 and T2 align images (but not for football, because there is no need). And then, I am a useful undressing skull and eliminate the cerebellum and brain T1 photo shoot using performs within the Organization. In this method, I can cover the brain without brain stalk skull and brain and the cerebellum [73, 79-82]. With this, the brain cover, finally separating the skull, the cerebellum and the brain also part of linked pictures that T2 and FA images. [95].

To create labor-intensive separation, a primary segmentation was acquired with widely existing kid brain separation software, IBEAT[96]. Then, physical elimination remained wisely accomplished using the practiced rater for modifying possible segmentation error according to the T1, T2 and FA images. For collaboratig physical elimination, ITK-SNAP is mostly used[97]. For each form of brain nourshing, usually, there are 100 axial slices. I chose arbitrarily sliced central areas for the manual chapter (slides 40-60). This project used these slides physically fragmented. Because I am not able to take pictures, we used only 2 FA images upcoming topics 8 left in this business. Note This pixel is preserved as models. For each topic, I have created over 10,000 points highlighted in each pixel images T1, T2 and FA. These points are measured as preparation and test models in my learning.

3.2.2 Brain Images Segmentation by DeepCNN for Multi-Modality

Deep learning procedure is a type of machine that may lean and grade of feature extraction by the structure of high –level to low-level ones. Deep models is a type of the convolutional neural networks (CNN) [97], in which trainable lattice and resident area merging procedures stay useful alternate input images on the rare, subsequent in the grading of gradually composite sorts. Single stuff of convolutional neural network (CNN) is its competency near detention extremely non –linear comparing among outputs and inputs. When accomplished with suitable regularization, convolutional neural networks (CNN) can succeed in the greater presentation on pictorial object appreciation and image classification jobs. In accumulation, convolutional neural networks (CNN) has also been used in insufficient other submissions. In [98] and [99] the volumetric electron microscopy images have segmented and bring back from functional convolutional neural networks (CNN). Functional deep CNN to distinguish histology mitosis breast images by using classifier pixel patches are established [100]. In this struggle, me use CNN suggest nourshing brain tissue segmentation, incorporating multiple T1, T2 images and method of FA. While CNN has used to work in previous revisions, none of them had focused on inclusion and integration of multi-modality method of image data. CNN only allow me in multiple entry maps similar to different methods of data, which provides common formalities to incorporate multiple data method. At the same time, the effectiveness of various methods including evidence interview, i were offered preliminary conclusions that combined multiple data checks of CNN enhance age exclusion. Structure of CNN Fig. 3.2 showed me create a confusion nursling brain images in white matter (WM) and gray matter (GM) cerebrospinal fluid (CSF).

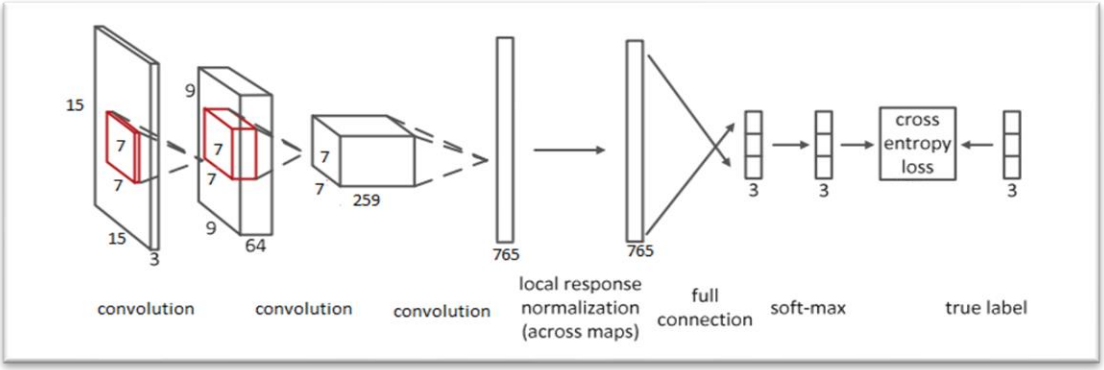

Figure 5. Patch size 15x15 is taken as input and its detailed structural design of the convolutional neural networks are obtained.

3.2.3 Deep Convolutional Neural Networks (CNN) Structural Design

In that proposed study, four convolutional neural networks (CNN) structural design has established on multi-modality MR images to segment the tissue of kids brain. In the following above, the CNN structural design provides detailed and to explain the system which is used in this work of the input patch size 15x15. The complete structural design has shown in Fig. 3.2. That convolutional neural networks (CNN) construction confined in three different feature maps which correspond to T1, T2, and FA images patches of 15x15. Then that's useful for three convolutional sheets and one sheet is fully associated. These networks too useful to softmax sheets and local reaction normalization.

First only 64 convolutional class characteristic plots. Both feature pieces associated with all three have plots more than 7 x 7 size filters. We used a single pixel stride size. This will create the maps feature size 9 x 9 in this layer. Layer another won first division convolution output as inputs and only 259 feature pieces. Two had associated attribute maps all maps feature in previous class made a size7 filters x 7. Again we use a pixel size pride. The third layer convolution 765 feature limited pieces 1 x 1. For all maps feature the previous layer of 7 x 7 filters. Me used a pixel pitch size also in this layer. In all of the repaired linear unit, the convolutional sheet has useful in the proposed convolutional procedure [101]. The use of ReLU may accelerate the training of CNN that has been exposed.

Apart from the documents convolutional, used certain types of extra paper at CNN. Specifically, the structure of normalization limited answer helpful after the third paper cut impose contrasts between identical spatial position through various feature. Successfully inserted layer Layer 3 normalization May outputs relating to three categories. Softmax 3-way paper used to create spread over 3 class Abel export later fully connected. Our network dropped damage divided between entropy prediction and brand truth crushed. Now adding, recycled failure to more learn vigorous types[102] and overfitting is decreased. This action put the production each neuron to zero with the possibility of 0.5, waster was useful earlier papers in relation to full geometry in fig. 3.2 CNN. In whole, that's trained limitations to amount on this structure 5.332.995. Also, the other three deliberated CNN planning with input patch design sizes 9 x 9 and 17 x 17 and 22 x 22. These CNN planning of convolution consists of convolutional sheet and change of feature strategies. Organization and local reactions softmax separately have practically in the structural design of the paper. I also pool mattress Max structural design with correct details size 22 x 22 after convolutional first sheet. Sarid size is set to 2 x 2 and 2 x 2 used for pooling size. Provided full information on these structural design in table 3-2. Trained for these amounts in structural design constraints are 6,577,155 and 5,947,523 and 5,332,995, in reoccurrence.

Table 3. In this table with different input patches size are explain of the CNN structural design in this effort. Full.com, Norm. and Conv. denotes fully- connected, normalisation and convolutional layers respectively.

Patchsize	Layer Detail	Layer1	Laye2	Laye3	Layer4	Layer5	Layer6	Layer7
9x9	Layer type #of feat.Map Filter size Conv. stride Input size	Conv. 259 7x7 1x1 9x9	Conv. 1024 7x7 1x1 7x7	Norm. 1024 _ _ 1x1	Full.com 3 1x1 1x1 1x1	Softmax 3 _ _ 1x1	_ -	-
15x15	Layer type #of feat. Map Filter size Conv. stride Input size	Conv. 64 7x7 1x1 15x15	Conv. 259 7x7 1x1 9x9	Conv. 765 7x7 1x1 7x7	Norm 765 _ _ 1x1	Full.com 3 1x1 1x1 1x1	Softmax 3 _ _ 1x1	-
17x17	Layer type #of feat. Map Filter size Conv.stride Input size	Conv. 64 7x7 1x1 17x17	Conv. 128 7x7 1x1 15x15	Conv. 256 7x7 1x1 9x9	Conv. 765 7x7 1x1 7x7	Norm. 765 _ _ 1x1	Full.com 3 1x1 1x1 1x1	Soft max 3 _ _ 1x1
22x22	Layer type #of feat. Map Filter size Pooling stride Pooling size Input size	Conv. 64 7x7 - _ 22x22	Poolig 64 _ 2x2 2x2 18x18	Conv. 259 7x7 _ _ 9x9	Conv. 765 7x7 _ _ 7x7	Norm. 765 _ _ _ 1x1	Full.com 3 1x1 _ _ 1x1	Soft max 3 _ _ _ 1x1

3.3 Data set

The dataset used for the research and experiment purpose has been collected from MRI center department of radiology and diagnostic imaging, Bahawal Victoria Hospital, Bahawalpur, Pakistan. This dataset consists of several brain tumor related disorder. However, in this research activity, three types of diseases have been classified. It contains 3000 brain tumor MRI images. The image was taken from 100 patients at different planes. The brain disorder classify in this research are Glioma, Meningioma, and Residual. For each subject of the glioma patient (1000 images), meningioma (1000 images) and residual (1000 images). There are three type of sequences, i.e., T1W, T2W, and FLAIR, each one has both of the orientations, i.e., axial and sagittal. Each sequence has 21 images, hence, each subject has a total of 126 images. Each image has a dimension of 512*512. There were total 7 subjects diagnosed with brain tumor of glioma. So, there were a total of 7*126=882 no of images. The proposed system utilized 1000 images for each of brain tumor type. To have 1000 images, for glioma, data augmentation has been used. For meningioma dataset of 10 patients has been used each patient contains 126 images and a total of 1260 MRI images has been used. For Residual, data set of 3 patients has been used in which each patients has 126 images and total 378 images used . We used 60% of the data for training purpose, 20% of the data for cross validation and 20% of the data for testing of the proposed system.

Preprocessing is optional step, there are several preprocessing related steps. In this study skull has been stripped as a preprocessing step.

For segmentation of tumor, in this research work, Fuzzy C mean algorithm has been used. The working fuzzy C mean algorithm has been described has under;

Fuzzy C mean is a data clustering method in which a data set is assembled into N clusters. In which each data point in the data set fitting to every cluster to a definite degree. Data point near to the center of a cluster have a high degree of connection and data point far from center of cluster have low degree of connection

$$\sum_{j=1}^{k}\sum_{x_i \in c_j} ui^m j(xi - \mu j)^2$$

Where,

- μij is the degree to which an observation xi belongs to a cluster *cj*
- μj is the center of the cluster *j*
- $\mu ij$is the degree to which an observation xi belongs to a cluster *cj*
- *m* is the fuzzifier.

Table 4: Showing Glioma, Meningioma and residual tumor images for each of available Sequences T1 Axial, T2 Axial, T2 Flair, T2 Axial, T2 Sagittal

-	Glioma	Meningioma	Residual
TI Axial			
T2 Axial			
Flair			

T2 Axial			
T2 Sagitial			

Table 5: Showing original and segmented image of Glioma

Original Image	Segmented Image
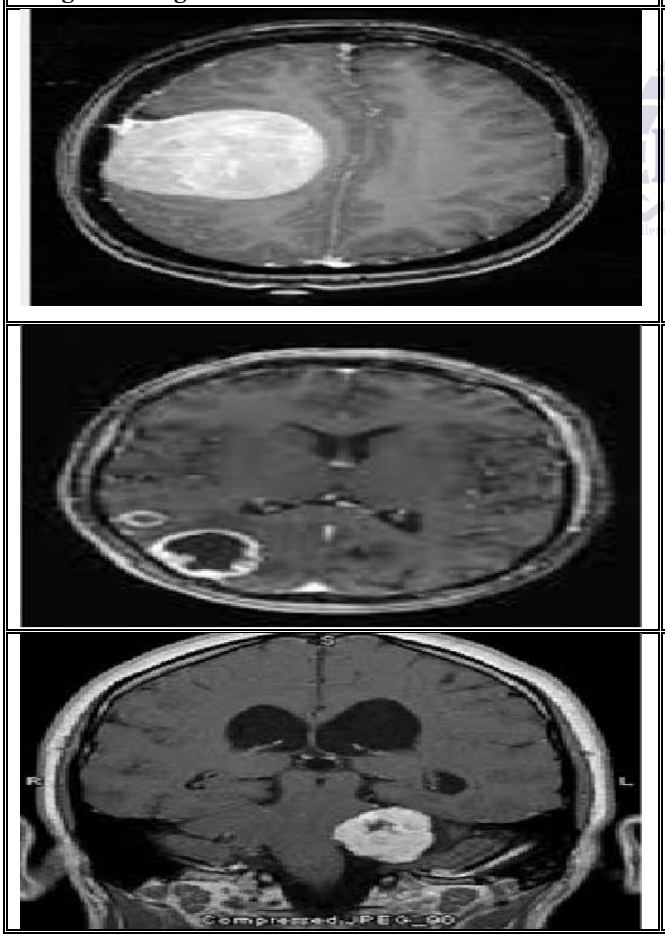	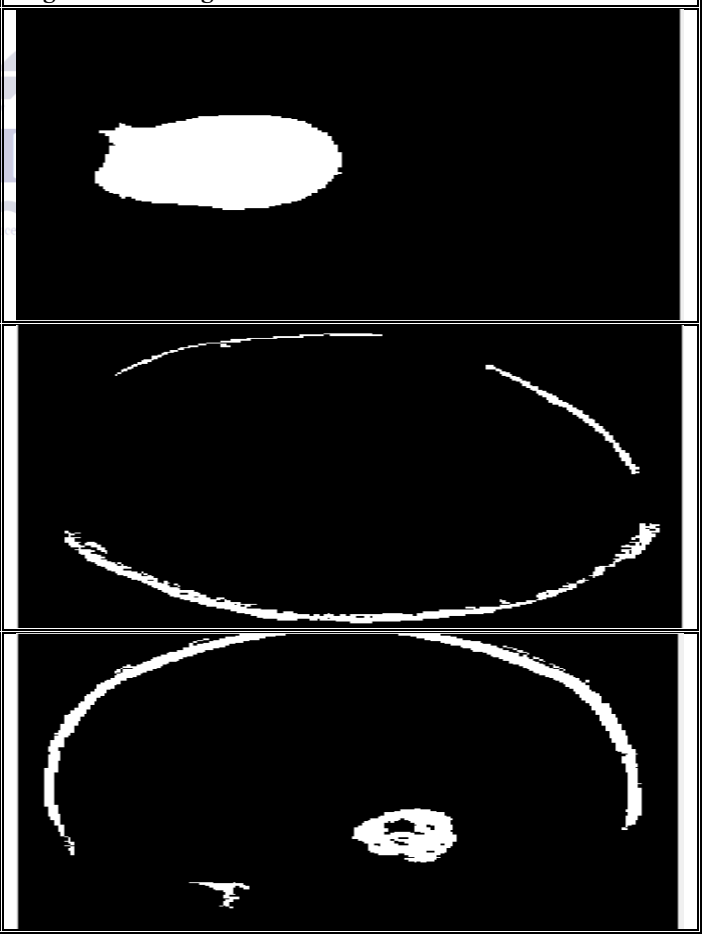

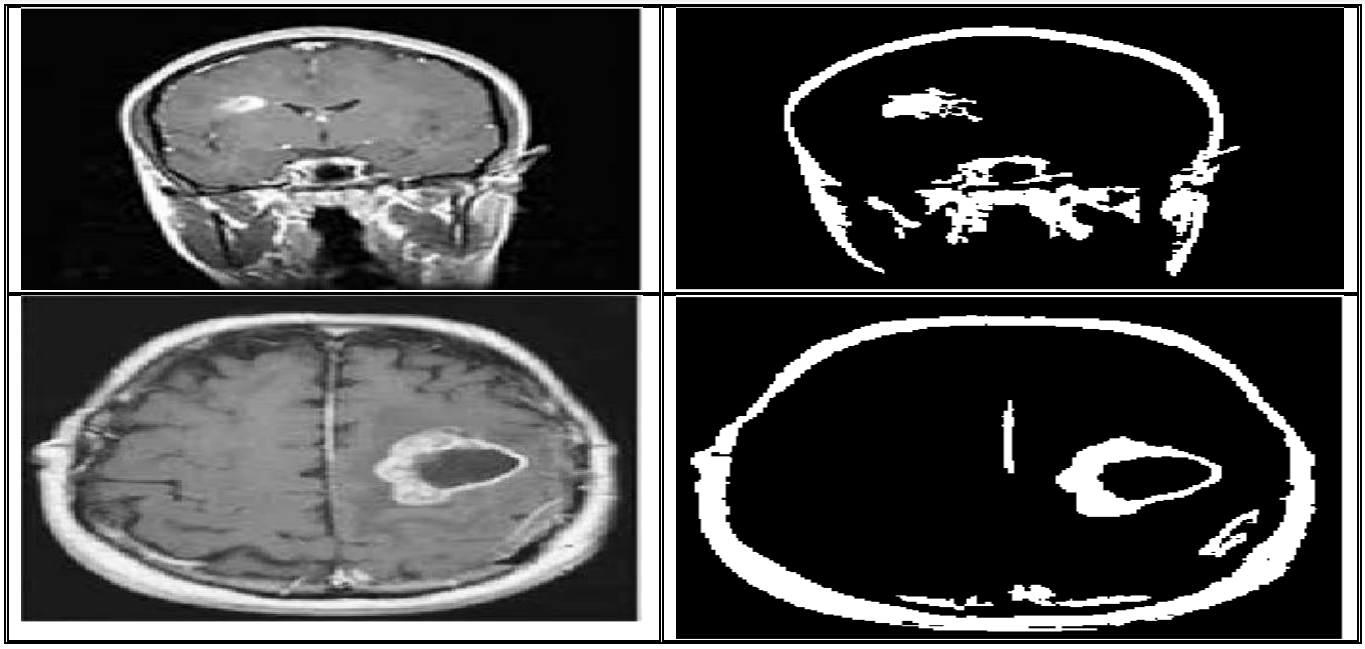

Table 6. Showing original and segmented image of Menigioma

Original Image	Segmented Image
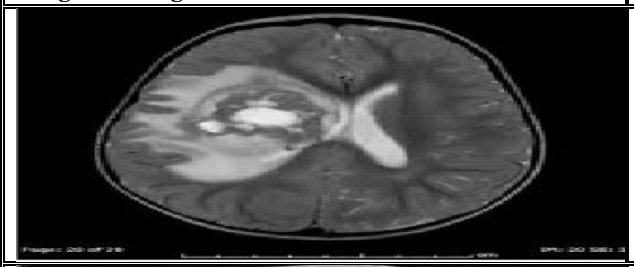	
	
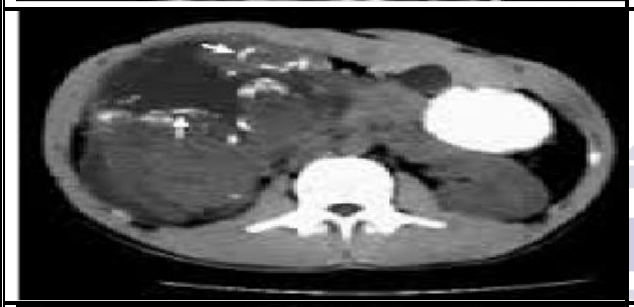	
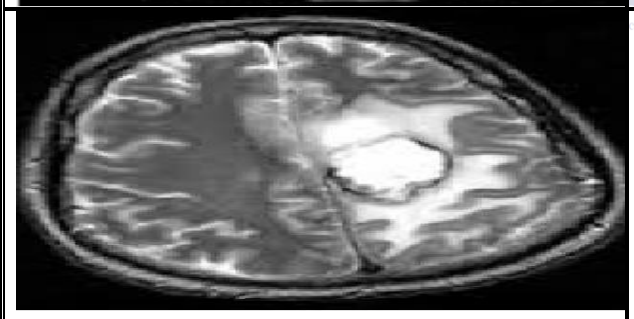	
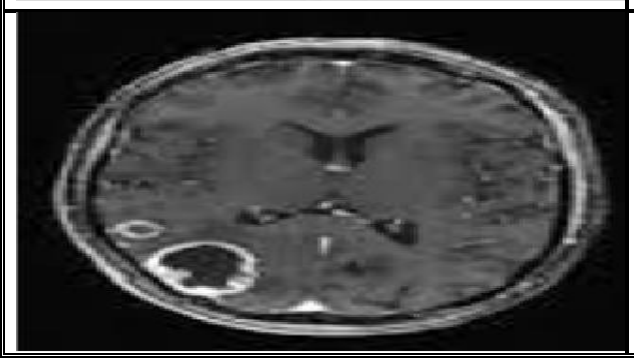	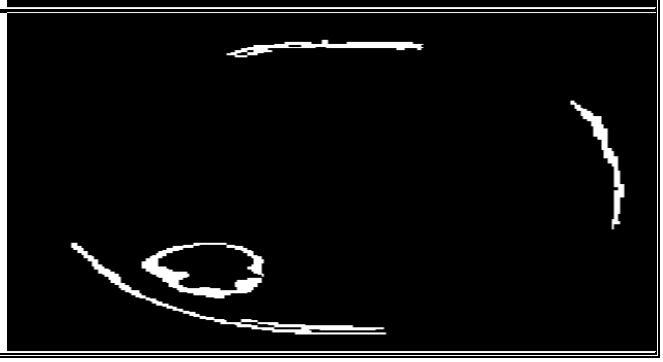

3.4 Classification of Brain tumor using Convolutional Neural network

Convolutional network is deep learning algorithm. It takes an input image allocate priority to different images and compare it with other.

3.4.1 Convolutional Layer

The essential preprocessing is lesser as associated with other algorithm. Convolutional's layer consist of set of constraints. Throughout the forward pass we slide every filter transversely to the height and width of input volume. When we slide the filter ended to the width and height then it produces 2 dimensional activation map.

3.4.2 Pooling Layer

It is common to add pooling layer in convolutional network. The pooling layer autonomously on every input depth slice. The most found is pooling with filter of 2x2 that is pragmatic with 2 down sample each depth slice input by 2 sideways both height and width and remove 75 % of the activation.

More generally, the pooling layer:

- Accepts a volume of size Width1×Height1×Dim1Width1×Height1×Dim1
- Requires two hyperparameters:
  - their spatial extent FF,
  - the stride SS,
- Produces a volume of size Width2×Height2×Dim2Width2×Height2×Dim2 where:
  - Width2=(Width1−F)/Str+1Width2=(Width1−F)/S+1
  - Height2=(Height1−F)/Str+1Height2=(Height1−F)/Str+1
  - Dim2=Dim1Dim2=Dim1
- It Introduces zero parameters later it calculates a fixed function of the input
- For Pooling layers, it is not common to pad the input using zero-padding.

3.4.3 Normalization Layer

Several type of normalization layer have been projected in CNN.

3.4.4 Fully Connected Layer

Neuron in a abundantly connected layer have full connection with previous layer. Their activation can be calculated with matrix by a bias offset.

4 RESULTS AND DISCUSSIONS

In this research, the dataset is collected from the Bahawal Victoria Hospital (BVH), Bahawalpur. Pakistan. This dataset is built using magnetic resonance images (MRI) images, which consists of different sequences and orientations.

In this research work, we have perfomred experiments in four different ways;

1. Processed data as it is, as scanned through MRI scanner
2. Processed extracted tumor region
3. Used data after proprocessing and data augmentation techniques
4. Used data after proprocessing and data augmentation techniques for glioma and meningioma

Results have been obtained from all six experimtns, which are as under;

4.1 Results obtained from Expeiment No 01

In this experiment, we used 1000 images for glioma case, 1000 for meningioma and 1000 for residual tumor . We used 750 images of each of these case for training data and rest of the images were used for testing data.

Data augmentation tool is used for making 1000 images of each category. The validation accuracy of this experiment was 66.13% and was completed in 68 iterations. The graph of accuracy and error rate per each epoch/iteration is shown in Figure 6. As this achieved accuracy is not up to the mark, to have this accuracy as acceptable we have performed further three experiments.

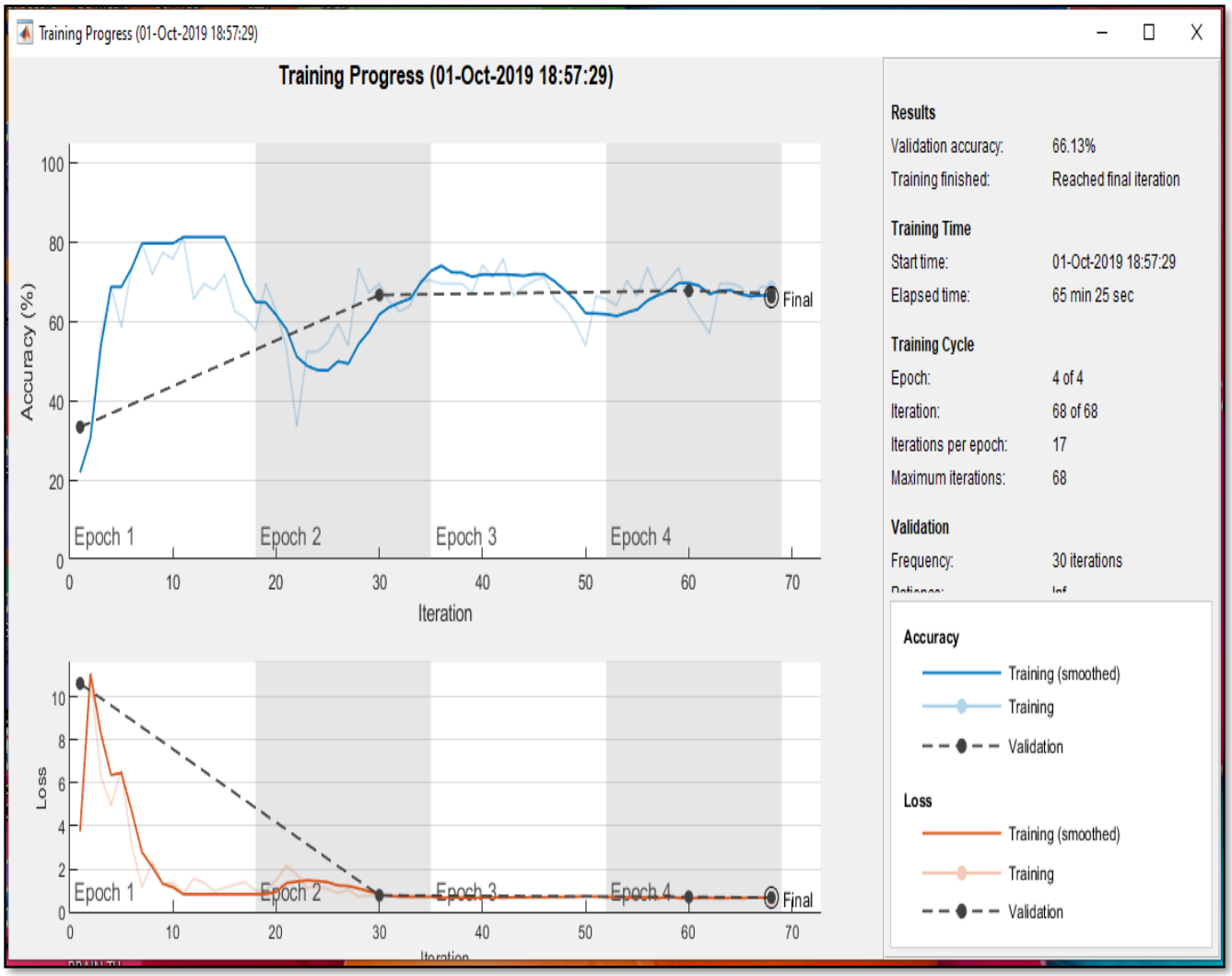

Figure 6: Graph of accuracy and error rate per epoch/iteration obtained during Experiment No. 01.

4.2 Results obtained from Expeiment No 02

In this experiment, we used 2000 images for glioma case, 2000 for meningioma and 2000 for residual tumor. We used 1500 images of each of these case for training data and rest of the images were used for testing data. Data augmentation tool has been used for making 2000 images of each category. The validation accuracy of this experiment was 80.93% on 68 iterations and 4 epochs. This accuracy is appriciative. The graph of accuracy and error rate per each epoch/iteration is shown in Figure 7.

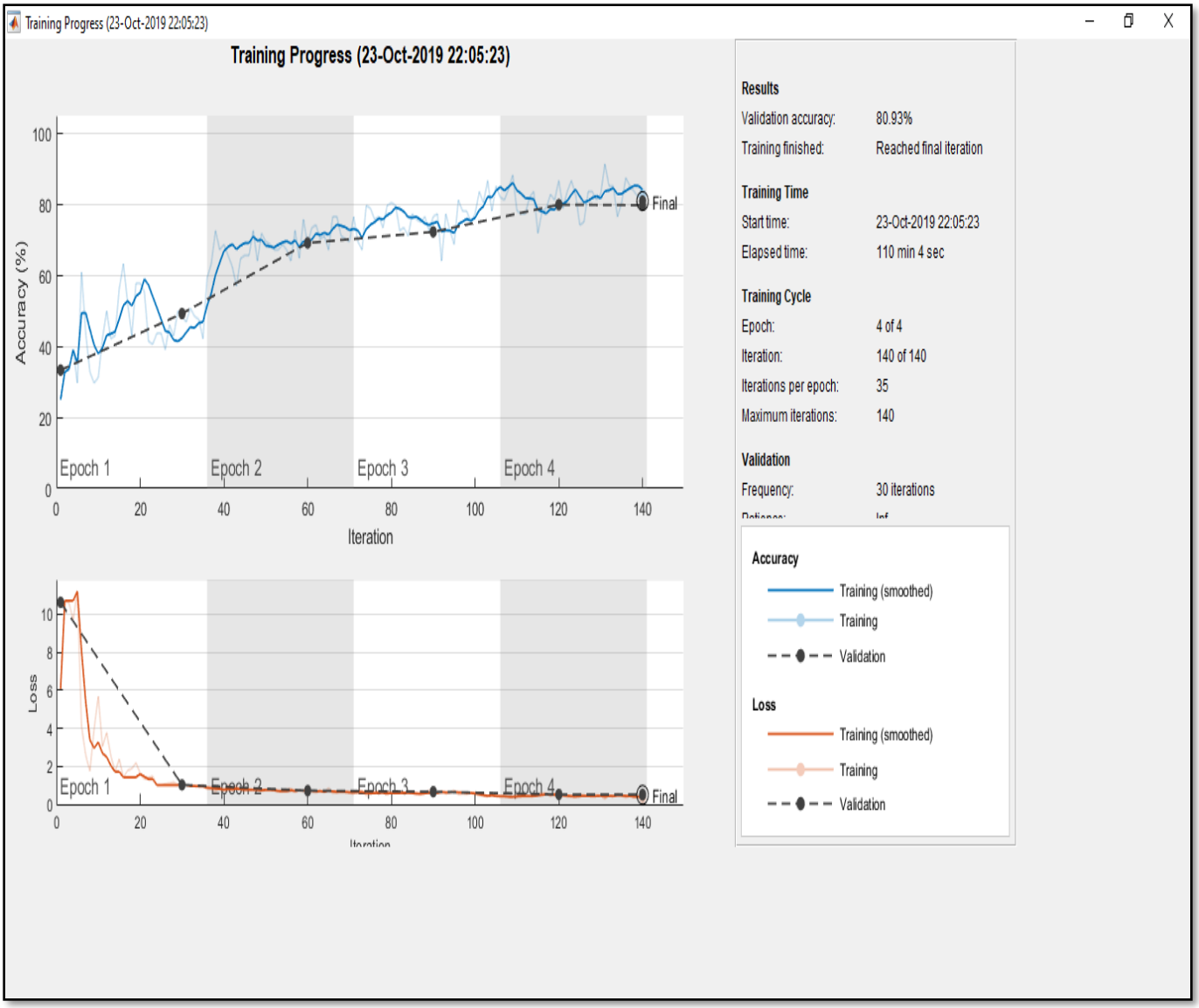

Figure 7: Graph of accuracy and error rate per epoch/iteration obtained during Experiment No. 02.

4.3 Results obtained from Expeiment No 03

In this experiment, we used 2000 images for glioma case, 2000 for meningioma and 2000 for residual tumor . We used 1500 images of each of these case for training data and rest of the images were used for testing data. Data augmentation tool has been used for making 2000 images of each category. The validation accuracy of this experiment was 88.07% on 68 iterations and 4 epochs. This accuracy is appriciative. The graph of accuracy and error rate per each epoch/iteration is shown in Figure 8.

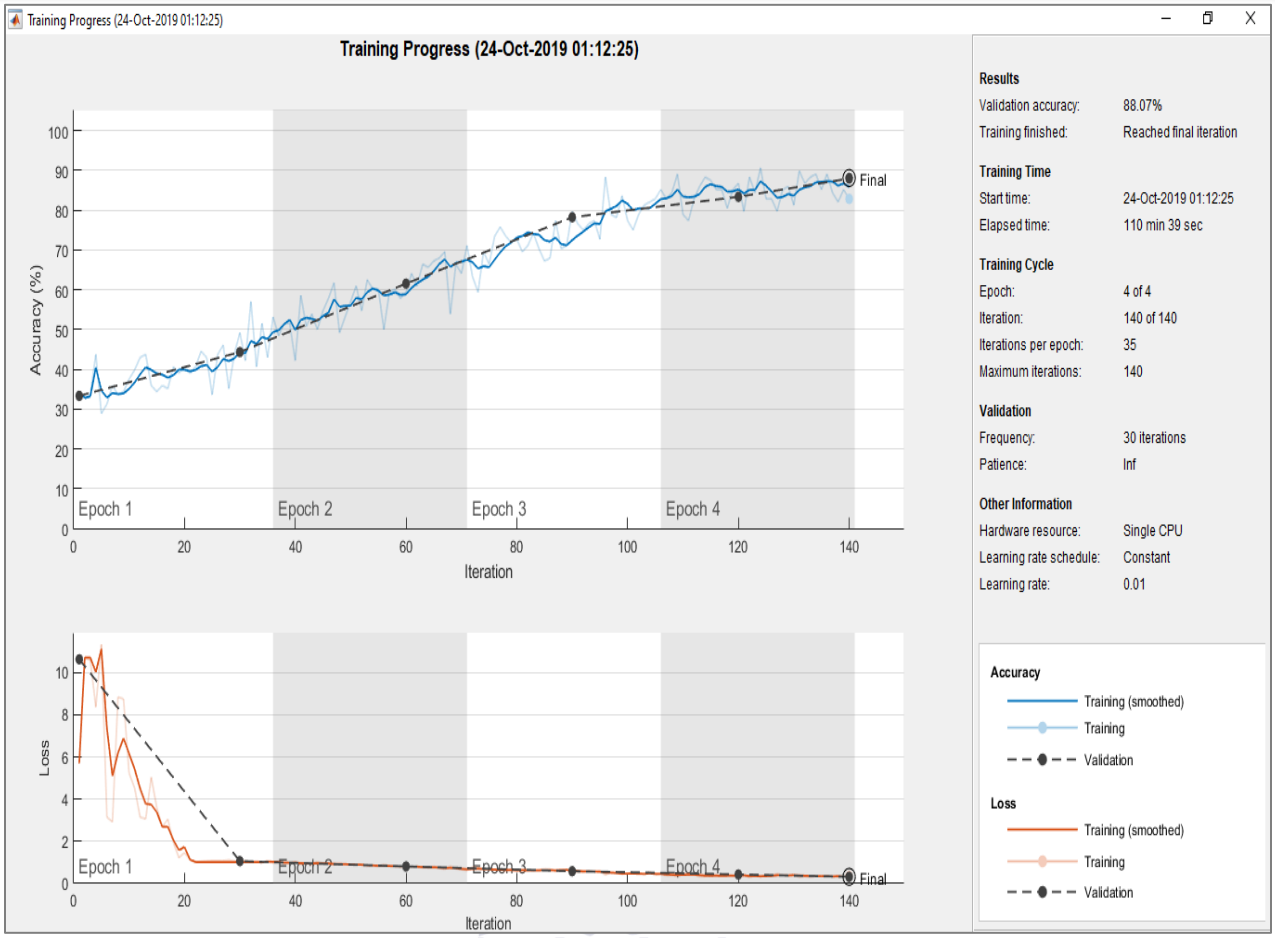

Figure 8: Graph of accuracy and error rate per epoch/iteration obtained during Experiment No. 03.

4.4 Results obtained from Expeiment No 04

In this experiment, we used 1000 images for glioma case, 1000 for meningioma and 1000 for residual tumor . We used 750 images of each of these case for training data and rest of the images were used for testing data. Data augmentation tool has been used for making 1000 images of each category. The validation accuracy of this experiment was 91.33% on 68 iterations and 4 epochs. This accuracy is appriciative. The graph of accuracy and error rate per each epoch/iteration is shown in Figure 9.

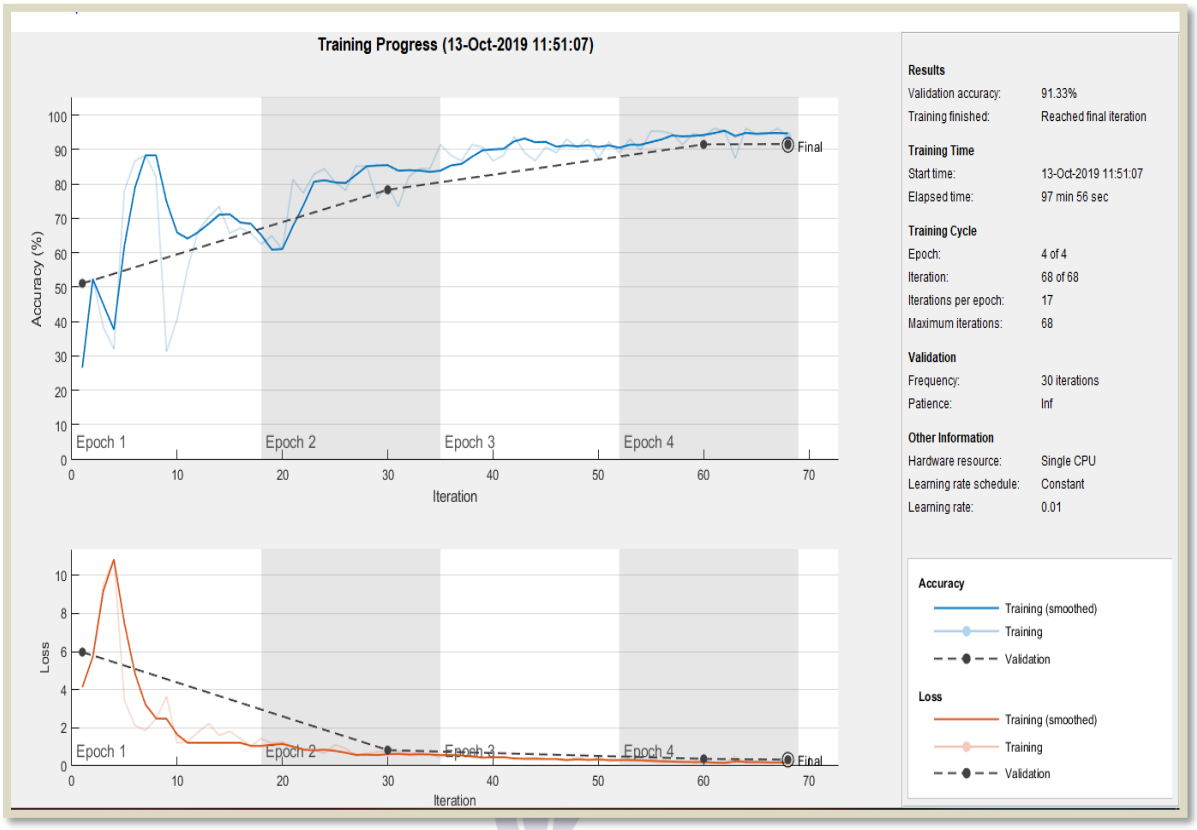

Figure 9: Graph of accuracy and error rate per epoch/iteration obtained during Experiment No. 04

4.5 Results obtained from Expeiment No 05

In this experiment, we used 1000 images for glioma case, 1000 for meningioma and 1000 for residual tumor . We used 750 images of each of these case for training data and rest of the images were used for testing data. Data augmentation tool has been used for making 1000 images of each category. The validation accuracy of this experiment was 92.00% on 68 iterations and 4 epochs. This accuracy is appriciative .The graph of accuracy and error rate per each epoch/iteration is shown in Figure 10.

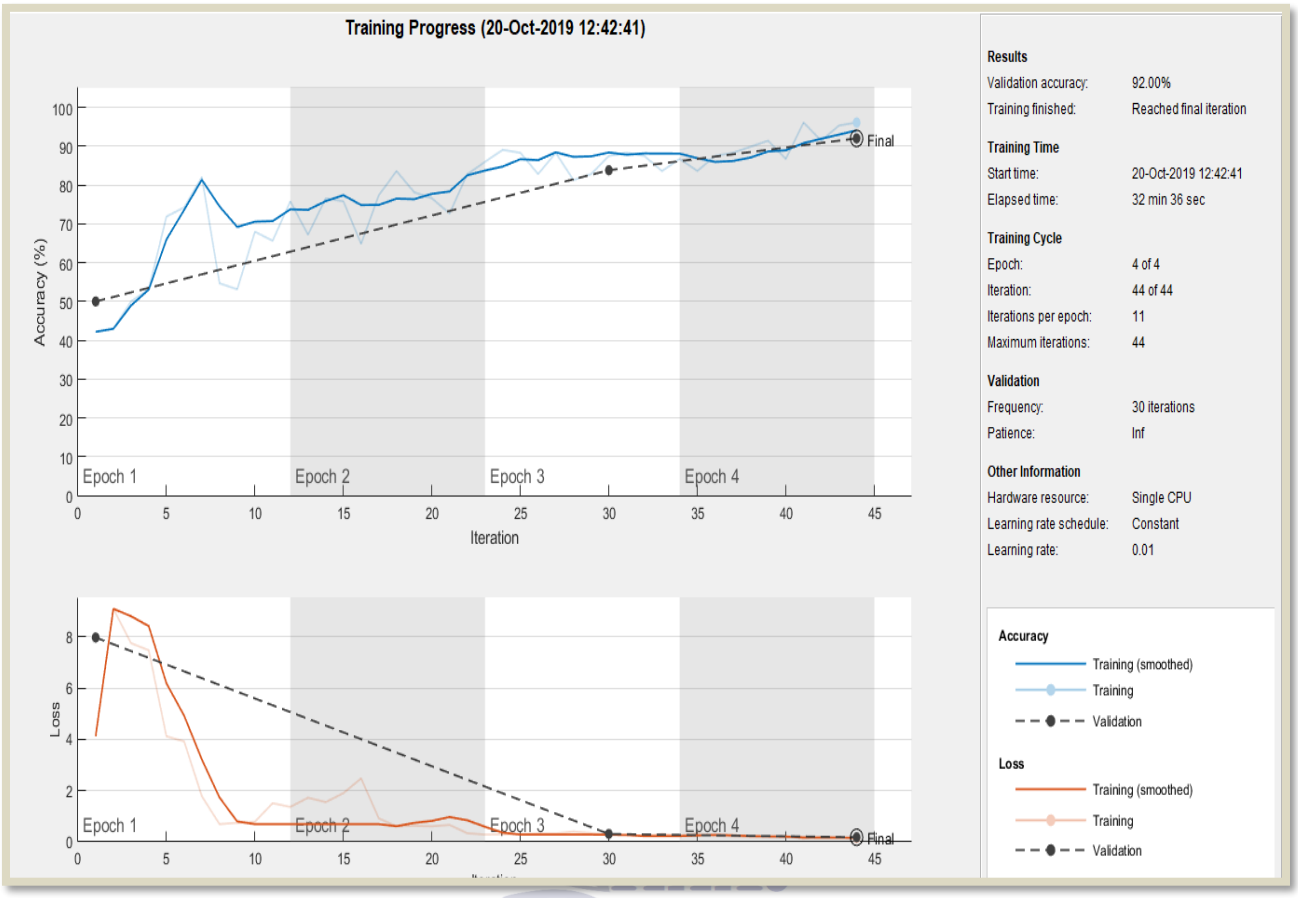

Figure 10: Graph of accuracy and error rate per epoch/iteration obtained during Experiment No. 05

4.6 Results obtained from Expeiment No 06

In this experiment, we used 1000 images for glioma case, 1000 for meningioma and 1000 for residual tumor . We used 750 images of each of these case for training data and rest of the images were used for testing data.

Data augmentation tool has been used for making 1000 images of each category. The validation accuracy of this experiment was 92.93% on 68 iterations and 4 epochs. This accuracy is appriciative and is highest accuracy achieved in this research work. The graph of accuracy and error rate per each epoch/iteration is shown in Figure 11.

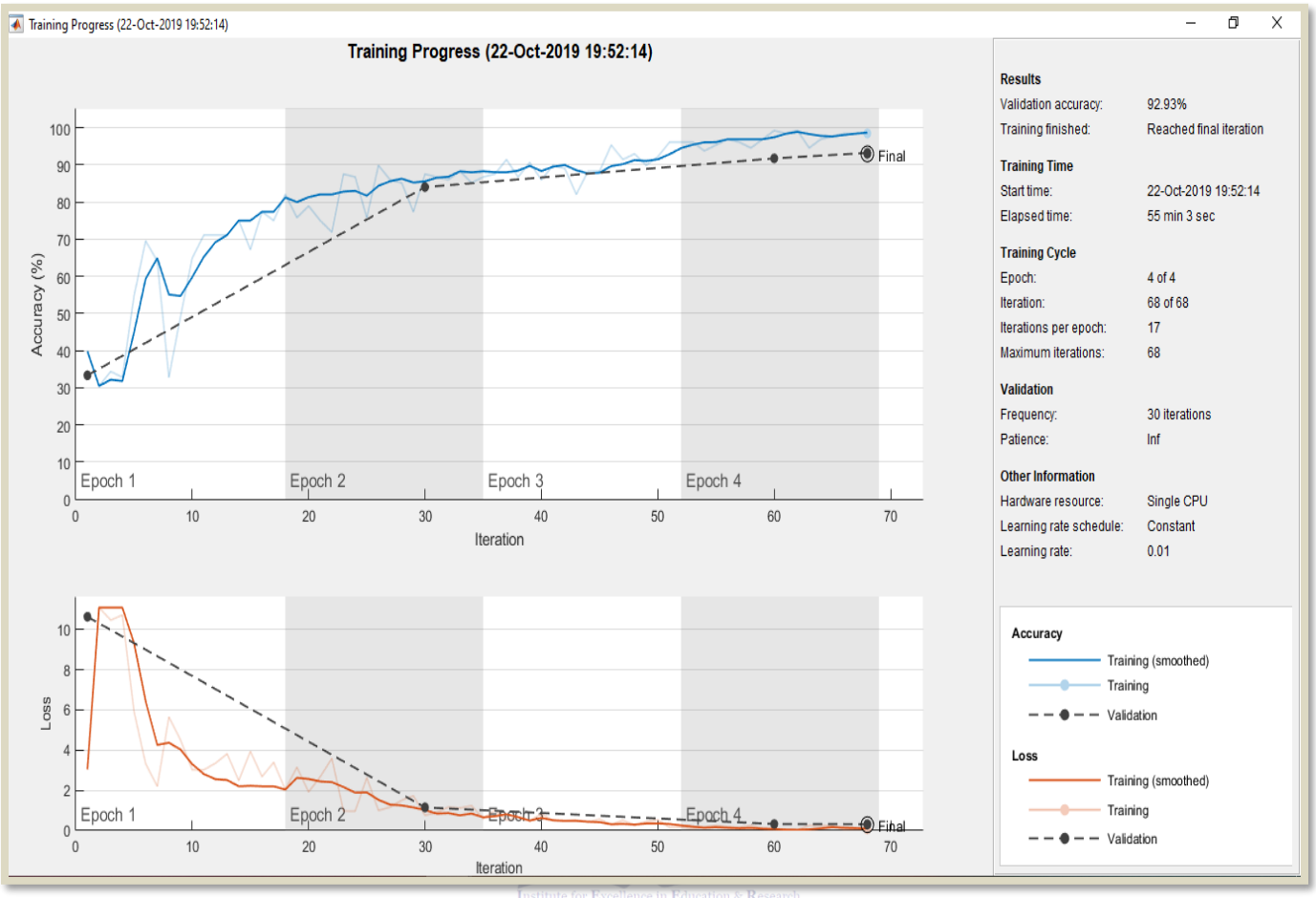

Figure 11: Graph of accuracy and error rate per epoch/iteration obtained during Experiment No. 06.

Table 7: Results obtained through the proposed model for different experiments

Sr#	Experiment No	No of Slices Used for	Accuracy
1	Experiment No.01	1000	66.13%
2	Experiment No.02	2000	80.93%
3	Experiment No.03	2000	88.07%
4	Experiment No.04	1000	91.33%
5	Experiment No.05	1000	92.00%
6	Experiment No.06	1000	92.93%

4.7 Discussions

Table 8 shows comparision of the results obtained through the proposed model with state-of-the-art methods performing brain tumor classification. The research activity conducted by Cheng, Jun, et al. [133], has addressed the problem of Menigioma, Glioma and Pitutary tumor classification with overall classification of 91.28%. Their proposed model used gray level co-occurenace method, SIFT features and SVM as a classifier. They used local datra set obtained from Nanfang Hospital,Guangzhou,China, and General Hospital, Tianjing Medical University, China. In another study conducted by J. S. Paul et al. [103] using deep learning has achived an overall accuracy of 72.13%. The experiments have also been performed on locaally developed dataset. Similarly, in another method reported by R. Zia et

al. [135] classified brain tumor on the dataset obtained from Harvard university with overall achieved accuracy of 85.69%, which is low. Similarly, M. Sajjad et al. [104] have classified brain tumor grades. The experimtns have been performed on locally developed datset with overall attained accurcy of 90.67%, which is a reasonable. In another recent study conducted by P. Afshar et al. [105], brain tumors have been classified against reported method with accuracy of 90.89%.

Table 9:Comparison with state-of-the-art methods

Sr. No.	Author, year	The proposed methodology	Dataset used	Classification of	Evaluation measures achieved
1.	Cheng, Jun, et al. [106], 2015	GLCM+SIFT+SVM	Locally developed dataset obtained from Nanfang Hospital,Guangzhou,China, and General Hospital, TianjingMedicalUniversity, China	Menigioma Glioma Pitutary tumor	91.28
2.	J. S. Paul et al. [103], 2017	Deep Learning	Locally developed dataset	Brain Tumor	72.13
3.	R. Zia et al. [107], 2018	DWT+PCA+SVM	Harvard University and from National Center for Image Guided Therapy	Brain Tumor Grades (II-IV)	85.69
4.	M. Sajjad et al. [104], 2019	Deep Learning	Locally developed dataset	Brain tumor Grade (I-IV)	90.67
5.	P. Afshar et al. [105], 2019	Capsule Network	Locally developed dataset	Three brain tumor types	90.89
6.	**The proposed**	**CNN**	**BVHB**	**Glioma, Menigioma, Residual**	**92.93**

Last row of Table 4 shows accuracy obtained from the proposed system. The proposed system achieved 92.93% accuracy, which as individually high as compared to the previously reported methods. The overall accuracy of our proposed system is a reasonable. The suggested approach overwhelmed existing approaches and achieved highest value of accuracy, i.e., 92.93%, which is the best results achieved so far as per our knowledge.

5 Conclusion

In this research work, a CNN based architecture has been proposed to classify brain tumor types Three classes, i.e., glioma, meningioma, and residual tumor have been classified. Otherwise in routine clinical environment, biopsy or spinal tape are the invasive methods used to determine a type of brain tumor. Experiments have been performed in three different ways, 1) processing of as it is images present in the dataset, 2) processing the tumor segmented images and 3) processing the large number tumor segmented images. Experiment no. 01, experiment no. 02 and

experiment no. 03 have achieved the accuracy as 79.40%, 92.40%, and 93.60% respectively. It has been experimentally proved that increasing the number of images has increased the achieved accuracy. In future work of this research work, all four WHO grades of brain tumor will be determined. It is further aimed that astrocytoma (the tumor present in astrocytes) will also be classified in its for WHO grades using non-invasive method to replace biopsy and spinal tape methods.

References

[1] E. A. Khera *et al.*, "Characterization of Nickel Oxide Thin Films for Smart Window Energy Conversion Applications: Comprehensive Experimental and Computational Study," *Available at SSRN 4235112*.

[2] M. Attique *et al.*, "Colorization and automated segmentation of human T2 MR brain images for characterization of soft tissues," *PloS one*, vol. 7, no. 3, p. e33616, 2012.

[3] H. Ullah, G. Gilanie, M. Attique, M. Hamza, and M. Ikram, "M-mode swept source optical coherence tomography for quantification of salt concentration in blood: an in vitro study," *Laser Physics*, vol. 22, pp. 1002-1010, 2012.

[4] G. Gilanie, "Spectroscopy of T2 weighted brain MR image for object extraction using prior anatomical knowledge based spectroscopic histogram analysis," 2013.

[5] G. Gilanie, M. Attique, S. Naweed, E. Ahmed, and M. Ikram, "Object extraction from T2 weighted brain MR image using histogram based gradient calculation," *Pattern Recognition Letters*, vol. 34, no. 12, pp. 1356-1363, 2013.

[6] H. Ullah, G. Gilanie, F. Hussain, and E. Ahmad, "Autocorrelation optical coherence tomography for glucose quantification in blood," *Laser Physics Letters*, vol. 12, no. 12, p. 125602, 2015.

[7] K. Asghar, G. Gilanie, M. Saddique, and Z. Habib, "Automatic Enhancement Of Digital Images Using Cubic BÃ© zier Curve And Fourier Transformation," *Malaysian Journal of Computer Science*, vol. 30, no. 4, pp. 300-310, 2017.

[8] H. U. Janjua, F. Andleeb, S. Aftab, F. Hussain, and G. Gilanie, "Classification of liver cirrhosis with statistical analysis of texture parameters," *International Journal of Optical Sciences*, vol. 3, no. 2, pp. 18-25, 2017.

[9] U. I. Bajwa, A. A. Shah, M. W. Anwar, G. Gilanie, and A. Ejaz Bajwa, "Computer-aided detection (CADe) system for detection of malignant lung nodules in CT slices-a key for early lung cancer detection," *Current Medical Imaging*, vol. 14, no. 3, pp. 422-429, 2018.

[10] G. Gilanie, U. I. Bajwa, M. M. Waraich, Z. Habib, H. Ullah, and M. Nasir, "Classification of normal and abnormal brain MRI slices using Gabor texture and support vector machines," *Signal, Image and Video Processing*, vol. 12, pp. 479-487, 2018.

[11] G. Gilanie, H. Ullah, M. Mahmood, U. I. Bajwa, and Z. Habib, "Colored Representation of Brain Gray Scale MRI Images to potentially underscore the variability and sensitivity of images," *Current Medical Imaging Reviews*, vol. 14, no. 4, pp. 555-560, 2018.

[12] H. U. Janjua, A. Jahangir, and G. Gilanie, "Classification of chronic kidney diseases with statistical analysis of textural parameters: a data mining technique," *International Journal of Optical Sciences*, vol. 4, no. 1, pp. 1-7, 2018.

[13] H. Ullah, A. Batool, and G. Gilanie, "Classification of Brain Tumor with Statistical Analysis of Texture Parameter Using a Data Mining Technique," *International Journal of Industrial Biotechnology and Biomaterials*, vol. 4, no. 2, pp. 22-36, 2018.

[14] G. Gilanie, U. I. Bajwa, M. M. Waraich, and Z. Habib, "Computer aided diagnosis of brain abnormalities using texture analysis of MRI images," *International Journal of Imaging Systems and Technology*, vol. 29, no. 3, pp. 260-271, 2019.

[15] A. Khursheed *et al.*, "A SMART HELMET TO DETECT ANOMALIES OF ITS USERS AND ENVIRONMENT," *Spectrum of Engineering Sciences*, vol. 4, no. 6, pp. 399-418, 2026.

[16] G. Gilanie, "Automated Detection and Classification of Brain Tumor from MRI Images using Machine Learning Methods," Department of Computer Science, COMSATS University Islamabad, Lahore campus, 2019.

[17] G. Gilanie, U. I. Bajwa, M. M. Waraich, and Z. Habib, "Automated and reliable brain radiology with texture analysis of magnetic resonance imaging and cross datasets validation," *International Journal of Imaging Systems and Technology*, vol. 29, no. 4, pp. 531-538, 2019.

[18] M. Amjad, H. Ullah, F. Andleeb, Z. Batool, A. Nazir, and G. Gilanie, "Fourier-Transform Infrared Spectroscopy (FTIR) for Investigation of Human Carcinoma and Leukaemia," *Lasers in Engineering (Old City Publishing)*, vol. 51, 2021.

[19] G. Gilanie, U. I. Bajwa, M. M. Waraich, and M. W. Anwar, "Risk-free WHO grading of astrocytoma using convolutional neural networks from MRI images," *Multimedia Tools and Applications*, vol. 80, no. 3, pp. 4295-4306, 2021.

[20] G. Gilanie *et al.*, "Coronavirus (COVID-19) detection from chest radiology images using convolutional neural networks," *Biomedical Signal Processing and Control*, vol. 66, p. 102490, 2021.

[21] G. Gilanie *et al.*, "RiceAgeNet: Age Estimation of Pakistani Grown Rice Seeds using Convolutional Neural Networks," *International Journal of Computational Intelligence in Control*, vol. 13, no. 2, pp. 831-843, 2021.

[22] G. Gilanie, N. Nasir, U. I. Bajwa, and H. Ullah, "RiceNet: convolutional neural networks-based model to classify Pakistani grown rice seed types," *Multimedia Systems*, pp. 1-9, 2021.

[23] G. Gilanie *et al.*, "Digital Image Processing for Ultrasound Images: A Comprehensive," *Digital Image Processing*, vol. 15, no. 3, 2021.

[24] S. Malik *et al.*, "Enhancing Contrast in Optical Imaging of Cancer tissues and Study the Spectral Properties of Methylene Blue," *Acta Microscópica*, vol. 30, no. 2, pp. 49-57, 2021.

[25] M. Rafiq, U. I. Bajwa, G. Gilanie, and W. Anwar, "Reconstruction of scene using corneal reflection," *Multimedia Tools and Applications*, pp. 1-17, 2021.

[26] A. A. Ghaffar *et al.*, "Refined Sentiment Analysis by Ensembling Technique of Stacking Classifier," in *International Conference on Soft Computing and Data Mining*, 2022, pp. 380-389: Springer.

[27] G. Gilanie *et al.*, "An Automated and Real-time Approach of Depression Detection from Facial Micro-expressions," *Computers, Materials & Continua*, vol. 73, no. 2, 2022.

[28] G. Gilanie, N. Rehman, U. I. Bajwa, S. Sharif, H. Ullah, and M. F. Mushtaq, "FERNet: A Convolutional Neural Networks Based Robust Model to Recognize Human Facial Expressions," in *International Conference on Soft Computing and Data Mining*, 2022, pp. 353-360: Springer.

[29] M. J. Iqbal, U. I. Bajwa, G. Gilanie, M. A. Iftikhar, and M. W. Anwar, "Automatic brain tumor segmentation from magnetic resonance images using superpixel-based approach," *Multimedia Tools And Applications*, vol. 81, no. 27, pp. 38409-38427, 2022.

[30] S. F. Rubab *et al.*, "The Comparative Performance of Machine Learning Models for COVID-19 Sentiment Analysis," in *International Conference on Soft Computing and Data Mining*, 2022, pp. 371-379: Springer.

[31] H. Ullah, M. Faran, Z. Batool, A. Nazir, G. Gilanie, and N. Amin, "Diagnosis of Ocular Diseases Using Optical Coherence Tomography (OCT) at λ= 840 nm," *Lasers in Engineering (Old City Publishing)*, vol. 53, 2022.

[32] E. Wazir, G. Gilanie, N. Rehman, H. Ullah, and M. F. Mushtaq, "Early Stage Detection of Cardiac Related Diseases by Using Artificial Neural Network," in *International Conference on Soft Computing and Data Mining*, 2022, pp. 361-370: Springer.

[33] M. Yaseen *et al.*, "In-vitro Evaluation of Anticancer Activity of Rhodamine-640 perchlorate on Rhabdomyosarcoma cell line," 2022.

[34] F. Afzal *et al.*, "Detection of Uric Acid in UV-VIS wavelength Regime," *JOURNAL OF NANOSCOPE (JN)*, vol. 4, no. 1, pp. 75-81, 2023.

[35] M. Ahmed, G. Gilanie, M. Ahsan, H. Ullah, and F. A. Sheikh, "Review of Artificial Intelligence-based COVID-19 Detection and A CNN-based Model to Detect Covid-19 from X-Rays and CT images," *VFAST Transactions on Software Engineering*, vol. 11, no. 2, pp. 100-112, 2023.

[36] S. Asghar *et al.*, "Water classification using convolutional neural network," *IEEE Access*, vol. 11, pp. 78601-78612, 2023.

[37] S. N. Batool and G. Gilanie, "CVIP-Net: A Convolutional Neural Network-Based Model for Forensic Radiology Image Classification," *Computers, Materials & Continua*, vol. 74, no. 1, 2023.

[38] M. Ghani and G. Gilanie, "The IOMT-Based Risk-Free Approach to Lung Disorders Detection from Exhaled Breath Examination," *INTELLIGENT AUTOMATION AND SOFT COMPUTING*, vol. 36, no. 3, pp. 2835-2847, 2023.

[39] G. Gilanie, U. I. Bajwa, M. M. Waraich, M. W. Anwar, and H. Ullah, "An automated and risk free WHO grading of glioma from MRI images using CNN," *Multimedia tools and applications*, vol. 82, no. 2, pp. 2857-2869, 2023.

[40] H. A. Hafeez *et al.*, "A CNN-model to classify low-grade and high-grade glioma from mri images," *IEEE Access*, vol. 11, pp. 46283-46296, 2023.

[41] E. A. Khera *et al.*, "Characterizing nickel oxide thin films for smart window energy conversion applications: Combined experimental and theoretical analyses," *ChemistrySelect*, vol. 8, no. 37, p. e202302320, 2023.

[42] A. Nazir, H. Ullah, G. Gilanie, S. Ahmad, Z. Batool, and A. Gadhi, "Exploring Breast Cancer Texture Analysis through Multilayer Neural Networks," *Scientific Inquiry and Review*, vol. 7, no. 3, pp. 32-47, 2023.

[43] H. Shafiq, G. Gilanie, M. Sajid, and M. Ahsan, "Dental radiology: a convolutional neural network-based approach to detect dental disorders from dental images in a real-time environment," *Multimedia Systems*, vol. 29, no. 6, pp. 3179-3191, 2023.

[44] H. Ullah *et al.*, "Proteins and Triglycerides Measurement in Blood Under Ultraviolet (UV)/Visible (Vis) Spectroscopy at & lambda;= 190 to 1100 nm with an Additional He-Ne Laser Source," *LASERS IN ENGINEERING*, vol. 55, no. 3-6, pp. 157-167, 2023.

[45] H. Ullah *et al.*, "Assessing Graphene Oxide (GO) and CuO Nanocomposites for Effective Antibacterial Properties Using Laser Interferometry," *Lasers in Engineering (Old City Publishing)*, vol. 55, 2023.

[46] H. Ullah, M. Zafar, Z. Batool, A. Nazir, G. Gilanie, and J. Rehman, "Early Detection of Liver, Ovary, Breast and Stomach Tumours in the Visible (λ= 630 nm) and Infrared (IR)(λ= 10.5 to 5.5 μm) Wavelength Regimes," *Lasers in Engineering (Old City Publishing)*, vol. 54, 2023.

[47] N. Abdullah, U. K. Ngah, and S. A. Aziz, "Image classification of brain MRI using support vector machine," in *Imaging Systems and Techniques (IST), 2011 IEEE International Conference on*, 2011, pp. 242-247: IEEE.

[48] J. K. Min *et al.*, "Age-and sex-related differences in all-cause mortality risk based on coronary computed tomography angiography findings: results from the International Multicenter CONFIRM (Coronary CT Angiography Evaluation for Clinical Outcomes: An International Multicenter Registry) of 23,854 patients without known coronary artery disease," *Journal of the American College of Cardiology*, vol. 58, no. 8, pp. 849-860, 2011.

[49] G. Gilanie *et al.*, "A Robust Method of Bipolar Mental Illness Detection from Facial Micro Expressions Using Machine Learning Methods," *Intelligent Automation & Soft Computing*, vol. 39, no. 1, 2024.

[50] S. Naveed *et al.*, "Drug efficacy recommendation system of glioblastoma (GBM) using deep learning," *IEEE Access*, 2024.

[51] M. S. Rashid, G. Gilanie, S. Naveed, S. Cheema, and M. Sajid, "Automated detection and classification of psoriasis types using deep neural networks from dermatology images," *Signal, Image and Video Processing*, vol. 18, no. 1, pp. 163-172, 2024.

[52] A. Saher, G. Gilanie, S. Cheema, A. Latif, S. N. Batool, and H. Ullah, "A Deep Learning-Based Automated Approach of Schizophrenia Detection from Facial Micro-Expressions," *Intelligent Automation & Soft Computing*, vol. 39, no. 6, 2024.

[53] H. ULLAH *et al.*, "Potential application of CeO2/Au nanoparticles as contrast agents in optical coherence tomography," *Journal of Optoelectronics and Advanced Materials*, vol. 26, no. July-August 2024, pp. 307-315, 2024.

[54] H. ULLAH *et al.*, "Measurements of Hyperproteinaemia in Human Blood Using Laser Interferometry: In Vitro Study," *Lasers in Engineering (Old City Publishing)*, vol. 57, 2024.

[55] W. Sun, B. Starly, J. Nam, and A. Darling, "Bio-CAD modeling and its applications in computer-aided tissue engineering," *Computer-aided design*, vol. 37, no. 11, pp. 1097-1114, 2005.

[56] M. Adnan *et al.*, "ETHNICITY CLASSIFICATION FROM FACIAL IMAGES USING DEEP LEARNING METHODS," *Spectrum of Engineering Sciences*, vol. 3, no. 9, pp. 1082-1156, 2025.

[57] A. Ahmed *et al.*, "ADAPTING IPV6 AND 6LOWPAN OVER WIFI-BASED AODV MANETS FOR IOT APPLICATIONS," *Spectrum of Engineering Sciences*, vol. 3, no. 7, pp. 1038-1052, 2025.

[58] M. Akhtar *et al.*, "Harnessing optics and statistics for early detection and prognosis in breast and ovarian cancer," *Lasers in Medical Science*, vol. 40, no. 1, p. 279, 2025.

[59] M. Amjad *et al.*, "Staging of Different Tumor by Utilizing Laser Guidance (@ 405 nm) in CT Scan Images Along with Statistical Analysis," *LASERS IN ENGINEERING*, vol. 59, no. 4-6, pp. 309-325, 2025.

[60] M. Amjad *et al.*, "Histopathology of Malignant Tissues Using High-Resolution Microscopy@ 630nm," *LASERS IN ENGINEERING*, vol. 59, no. 4-6, pp. 295-308, 2025.

[61] M. Anwaar, G. Gilanie, A. Namoun, and W. Sharif, "Optimizing Document Classification Using Modified Relative Discrimination Criterion and RSS-ELM Techniques," *International Journal of Advanced Computer Science & Applications*, vol. 16, no. 4, 2025.

[62] S. N. Batool *et al.*, "Forensic Radiology: A robust approach to biological profile estimation from bone image analysis using deep learning," *Biomedical Signal Processing and Control*, vol. 105, p. 107661, 2025.

[63] G. Gilanie *et al.*, "A ROBUST CONVOLUTIONAL NEURAL NETWORK-BASED APPROACH FOR HUMAN EMOTION CLASSIFICATION: CROSS-DATASET VALIDATION AND GENERALIZATION," *Spectrum of Engineering Sciences*, vol. 3, no. 4, pp. 782-798, 2025.

[64] G. Gilanie *et al.*, "A ROBUST ARTIFICIAL NEURAL NETWORK APPROACH FOR EARLY DETECTION OF CARDIAC DISEASES," *Spectrum of Engineering Sciences*, vol. 3, no. 4, pp. 499-511, 2025.

[65] G. Gilanie *et al.*, "DEEP LEARNING-BASED APPROACH FOR ESTIMATING THE AGE OF PAKISTANI-GROWN RICE SEEDS," *Spectrum of Engineering Sciences*, vol. 3, no. 1, pp. 557-572, 2025.

[66] G. Gilanie *et al.*, "STEGANOGRAPHIC SECRET COMMUNICATION USING RGB PIXEL ENCODING AND CRYPTOGRAPHIC SECURITY," *Spectrum of Engineering Sciences*, vol. 3, no. 3, pp. 323-336, 2025.

[67] G. Gilanie *et al.*, "READABLE TEXT RETRIEVAL FROM NOISE-INFLUENCED DOCUMENTS USING IMAGE RESTORATION METHODS," *Spectrum of Engineering Sciences*, vol. 3, no. 3, pp. 337-360, 2025.

[68] G. Gilanie *et al.*, "PARAMETER OPTIMIZATION OF AUTOENCODER FOR IMAGE CLASSIFICATION USING GENETIC ALGORITHM," *Spectrum of Engineering Sciences*, vol. 3, no. 4, pp. 201-213, 2025.

[69] A. Kashif *et al.*, "FORENSIC RADIOLOGY: AN INTELLIGENT METHOD OF AGE AND GENDER ESTIMATION FROM X-RAY SCANNED BONES IMAGES USING CONVOLUTIONAL NEURAL NETWORKS," *Spectrum of Engineering Sciences*, vol. 3, no. 7, pp. 440-487, 2025.

[70] A. Latif *et al.*, "A VISION-FREE OBSTACLE DETECTION AND ALERT SYSTEM USING SMART KNEE GLOVES," *Spectrum of Engineering Sciences*, vol. 3, no. 6, pp. 816-829, 2025.

[71] M. Sajid *et al.*, "IoMT-Enabled Noninvasive Lungs Disease Detection and Classification Using Deep Learning-Based Analysis of Lungs Sounds," *International Journal of Advanced Computer Science & Applications*, vol. 16, no. 2, 2025.

[72] M. A. Siddique *et al.*, "A Multi-Modal Approach for Exploring Sarcoma and Carcinoma Using FTIR and Polarimetric Analysis," *Microscopy Research and Technique*, 2025.

[73] J. Yang *et al.*, "BrainCNN: Automated Brain Tumor Grading from Magnetic Resonance Images Using a Convolutional Neural Network-Based Customized Model," *SLAS Technology*, p. 100334, 2025.

[74] M. Vaidyanathan, R. Velthuizen, L. Clarke, and L. Hall, "Quantitation of brain tumor in MRI for treatment planning," in *Engineering in Medicine and Biology Society, 1994. Engineering Advances: New Opportunities for Biomedical Engineers. Proceedings of the 16th Annual International Conference of the IEEE*, 1994, vol. 1, pp. 555-556: IEEE.

[75] G. Vezina, "MR Imaging of Brain Tumors-Recent Developments," *MD Director of Neuroradiology-Children's National Medical Center, Washington DC*, 2002.

[76] D. J. Werring *et al.*, "Cognitive dysfunction in patients with cerebral microbleeds on T2*-weighted gradient-echo MRI," *Brain*, vol. 127, no. 10, pp. 2265-2275, 2004.

[77] M. N. Tahir, "Classification and characterization of brain tumor MRI by using gray scaled segmentation and DNN," 2018.

[78] H. Kato, M. Izumiyama, K. Izumiyama, A. Takahashi, and Y. Itoyama, "Silent cerebral microbleeds on T2*-weighted MRI: correlation with stroke subtype, stroke recurrence, and leukoaraiosis," *Stroke*, vol. 33, no. 6, pp. 1536-1540, 2002.

[79] A. Farooq *et al.*, "CONCEPTUAL FRAMEWORK FOR AN EEG-DRIVEN HUMAN BRAIN INTERFACE FOR NEURAL ENCODING AND DECODING," *Spectrum of Engineering Sciences*, vol. 4, no. 5, pp. 2419-2435, 2026.

[80] M. Iqbal *et al.*, "Automated Identification of Mango Leaf Diseases Using Deep Convolutional Neural Networks," *Polish Journal of Environmental Studies*, 2026.

[81] M. Sajid *et al.*, "Internet of Medical Things-Driven Deep Learning Approach for Automated Heart Sound Classification," *IET Biometrics*, vol. 2026, no. 1, p. 3212328, 2026.

[82] M. Yasir, F. Siddique, F. Andleeb, G. Gilanie, and H. Ullah, "Differentiation of metastatic and primary brain tumor using magnetic resonance imaging," *International Journal of Radiation Research*, vol. 24, no. 1, pp. 259-265, 2026.

[83] S. Shah and N. Chauhan, "Classification of brain MRI images using computational intelligent techniques," *International journal of computer applications*, vol. 124, no. 14, 2015.

[84] A. Damayanti and I. Werdiningsih, "Classification of tumor based on magnetic resonance (MR) brain images using wavelet energy feature and neuro-fuzzy model," in *Journal of Physics: Conference Series*, 2018, vol. 974, p. 012027: IOP Publishing.

[85] J. Naik and S. Patel, "Tumor detection and classification using decision tree in brain MRI," *International Journal of Computer Science and Network Security (IJCSNS)*, vol. 14, no. 6, p. 87, 2014.

[86] K. Usman and K. Rajpoot, "Brain tumor classification from multi-modality MRI using wavelets and machine learning," *Pattern Analysis and Applications*, vol. 20, no. 3, pp. 871-881, 2017.

[87] J. Fink, D. Born, and M. C. Chamberlain, "Radiation necrosis: relevance with respect to treatment of primary and secondary brain tumors," *Current neurology and neuroscience reports*, vol. 12, no. 3, pp. 276-285, 2012.

[88] M. Havaei *et al.*, "Brain tumor segmentation with deep neural networks," *Medical image analysis*, vol. 35, pp. 18-31, 2017.

[89] K. Rezaei and H. Agahi, "SEGMENTATION AND CLASSIFICATION OF BRAIN TUMOR CT IMAGES USING SVM WITH WEIGHTED KERNEL WIDTH," *Computer Science & Information Technology*, p. 39.

[90] G. Litjens *et al.*, "A survey on deep learning in medical image analysis," *Medical image analysis*, vol. 42, pp. 60-88, 2017.

[91] M. J. Durán, S. Gallardo, S. L. Toral, R. Martínez-Torres, and F. J. Barrero, "A learning methodology using Matlab/Simulink for undergraduate electrical engineering courses attending to learner satisfaction outcomes," *International Journal of Technology and Design Education*, vol. 17, no. 1, pp. 55-73, 2007.

[92] N. B. Bahadure, A. K. Ray, and H. P. Thethi, "Image analysis for MRI based brain tumor detection and feature extraction using biologically inspired BWT and SVM," *International journal of biomedical imaging*, vol. 2017, 2017.

[93] R. N. Strickland, *Image-processing techniques for tumor detection*. CRC Press, 2002.

[94] D. Grady *et al.*, "Cardiovascular disease outcomes during 6.8 years of hormone therapy: Heart and Estrogen/progestin Replacement Study follow-up (HERS II)," *Jama*, vol. 288, no. 1, pp. 49-57, 2002.

[95] L. Wang, F. Shi, P.-T. Yap, J. H. Gilmore, W. Lin, and D. Shen, "4D multi-modality tissue segmentation of serial infant images," *PloS one*, vol. 7, no. 9, p. e44596, 2012.

[96] S. H. Kim *et al.*, "Adaptive prior probability and spatial temporal intensity change estimation for segmentation of the one-year-old human brain," *Journal of neuroscience methods*, vol. 212, no. 1, pp. 43-55, 2013.

[97] P. A. Yushkevich *et al.*, "User-guided 3D active contour segmentation of anatomical structures: significantly improved efficiency and reliability," *NeuroImage*, vol. 31, no. 3, pp. 1116-1128, 2006.

[98] V. Jain and S. Seung, "Natural image denoising with convolutional networks," in *Advances in Neural Information Processing Systems*, 2009, pp. 769-776.

[99] M. Helmstaedter, K. L. Briggman, S. C. Turaga, V. Jain, H. S. Seung, and W. Denk, "Connectomic reconstruction of the inner plexiform layer in the mouse retina," *Nature*, vol. 500, no. 7461, p. 168, 2013.

[100] A. Giusti, D. C. Ciresan, J. Masci, L. M. Gambardella, and J. Schmidhuber, "Fast image scanning with deep max-pooling convolutional neural networks," in *Image Processing (ICIP), 2013 20th IEEE International Conference on*, 2013, pp. 4034-4038: IEEE.

[101] V. Nair and G. E. Hinton, "Rectified linear units improve restricted boltzmann machines," in *Proceedings of the 27th international conference on machine learning (ICML-10)*, 2010, pp. 807-814.

[102] G. E. Hinton, N. Srivastava, A. Krizhevsky, I. Sutskever, and R. R. Salakhutdinov, "Improving neural networks by preventing co-adaptation of feature detectors," *arXiv preprint arXiv:1207.0580*, 2012.

[103] J. S. Paul, A. J. Plassard, B. A. Landman, and D. Fabbri, "Deep learning for brain tumor classification," in *Medical Imaging 2017: Biomedical Applications in Molecular, Structural, and Functional Imaging*, 2017, vol. 10137, p. 1013710: International Society for Optics and Photonics.

[104] M. Sajjad, S. Khan, K. Muhammad, W. Wu, A. Ullah, and S. W. Baik, "Multi-grade brain tumor classification using deep CNN with extensive data augmentation," *Journal of computational science*, vol. 30, pp. 174-182, 2019.

[105] P. Afshar, K. N. Plataniotis, and A. Mohammadi, "Capsule Networks for Brain Tumor Classification Based on Mri Images and Coarse Tumor Boundaries," in *ICASSP 2019-2019 IEEE International Conference on Acoustics, Speech and Signal Processing (ICASSP)*, 2019, pp. 1368-1372: IEEE.

[106] J. Cheng *et al.*, "Enhanced performance of brain tumor classification via tumor region augmentation and partition," *PloS one*, vol. 10, no. 10, p. e0140381, 2015.

[107] R. Zia, P. Akhtar, and A. Aziz, "A new rectangular window based image cropping method for generalization of brain neoplasm classification systems," *International Journal of Imaging Systems and Technology*, vol. 28, no. 3, pp. 153-162, 2018.